第71回日本血液学会学術集会
シンポジウム10
骨髄不全症候群の分子病態

テロメア関連遺伝子異常による骨髄不全症

山口博樹，　檀　和夫

Key words: Bone marrow failure, Dyskeratosis congenita, Telomerase complex gene, Telomere-associated shelterin protein complex gene

はじめに

テロメアは染色体の末端部位に存在する繰り返し配列をもつDNA（ヒトでは5'-TTAGGG-3'）とそこに局在するテロメラーゼ複合体やShelterin複合体などの種々のタンパク質から構成されている[1]。テロメアはその構造から他の要因で受けたDNA切断末端と区別され，DNAの分解や修復から染色体を保護し，物理的および遺伝的な安定性を保つ働きをしている[1]。

ヒトなどの動物組織から取り出した培養細胞は，複数回の分裂を繰り返すとテロメア長が短縮化し細胞分裂が停止する細胞老化という現象が認められる[2,3]。これは細胞分裂の際にDNA複製が行われるが，リーディング鎖は完全にコピーされるのに対して，ラギング鎖は最終の岡崎フラグメントから約200bp離れたところに複製のためのプライマーが合成されるため，3'末端の一部はコピーが不完全となるためである[1,4,5]。また仮に偶然3'末端にプライマーが合成されても，複製後プライマーはDNAに変換されないためテロメアの短縮化は避けられない[1,4,5]。しかし造血幹細胞や生殖細胞などでは，テロメラーゼによるテロメア長の伸長補正が行われるため常に細胞分裂が可能である[1]。

近年このテロメア長の伸長補正の障害が，Dyskeratosis congenita（DKC），一部の再生不良性貧血や骨髄異形性症候群，特発性肺線維症の原因と同定され，そして猫鳴き症候群，急性骨髄性白血病，肝硬変などの病態への関与も示唆されている[6~9]。本稿では，テロメア長の伸長補正の障害とDKCなどの骨髄不全症に関して概説する。

日本医科大学　血液内科

DKCにおけるテロメア関連遺伝子異常

DKCは網状色素沈着，爪の萎縮，舌などの粘膜白斑症を伴う骨髄不全症（Bone marrow failure: BMF）で10歳前後までに約80%以上の症例にこれらの特徴的身体所見が付随しBMFを発症する（図1）[7]。そして上記以外にも精神発育遅滞，肺疾患，低身長，歯の異常，食道狭窄，頭髪の喪失，白髪などの多彩な合併症が15～25%の症例に認められ，また8%の症例に皮膚，上咽頭，消化管の扁平上皮癌や腺癌などの悪性腫瘍や，骨髄異形性症候群，Hodgkin病，急性骨髄性白血病などの造血器腫瘍の発生が認められる[7]。

遺伝型式はX連鎖劣性遺伝が約35%，常染色体優性遺伝が約15%，常染色体劣性遺伝が数%に認められるが，残りの約40%近くが型式不明である[7]。近年テロメラーゼ複合体を構成する遺伝子群である，*DKC1*，*telomerase RNA component*（*TERC*），*telomerase reverse transcriptase*（*TERT*），*NOP10*，*NHP2*，またShelterin複合体を構成する*TRF-interacting nuclear protein*（*TINF2*）がDKCの責任遺伝子として同定された（表1）[6~9]。DKCはこれらの遺伝子の変異によりテロメアが短縮し，その結果造血幹細胞などの増殖能に障害が起き上記の症候が形成されると考えられている[7]。

またDKCの発症年齢，随伴症状，造血障害の有無とテロメアの短縮化の程度には相関がみられ，後述のDKCの重症型と考えられているHoyeraal-Hreidarsson syndrome（HHS）はDKCと比較してテロメアの短縮が著しいと報告されている[10]。

HHSは男児の幼時期に骨髄不全症を発症する遺伝性疾患である。骨髄不全症以外には小頭症，小脳低形成，成長発達遅延，顔貌異常，B細胞とNK細胞数の低下，細胞性免疫不全を合併し大多数の症例は10歳前後で死

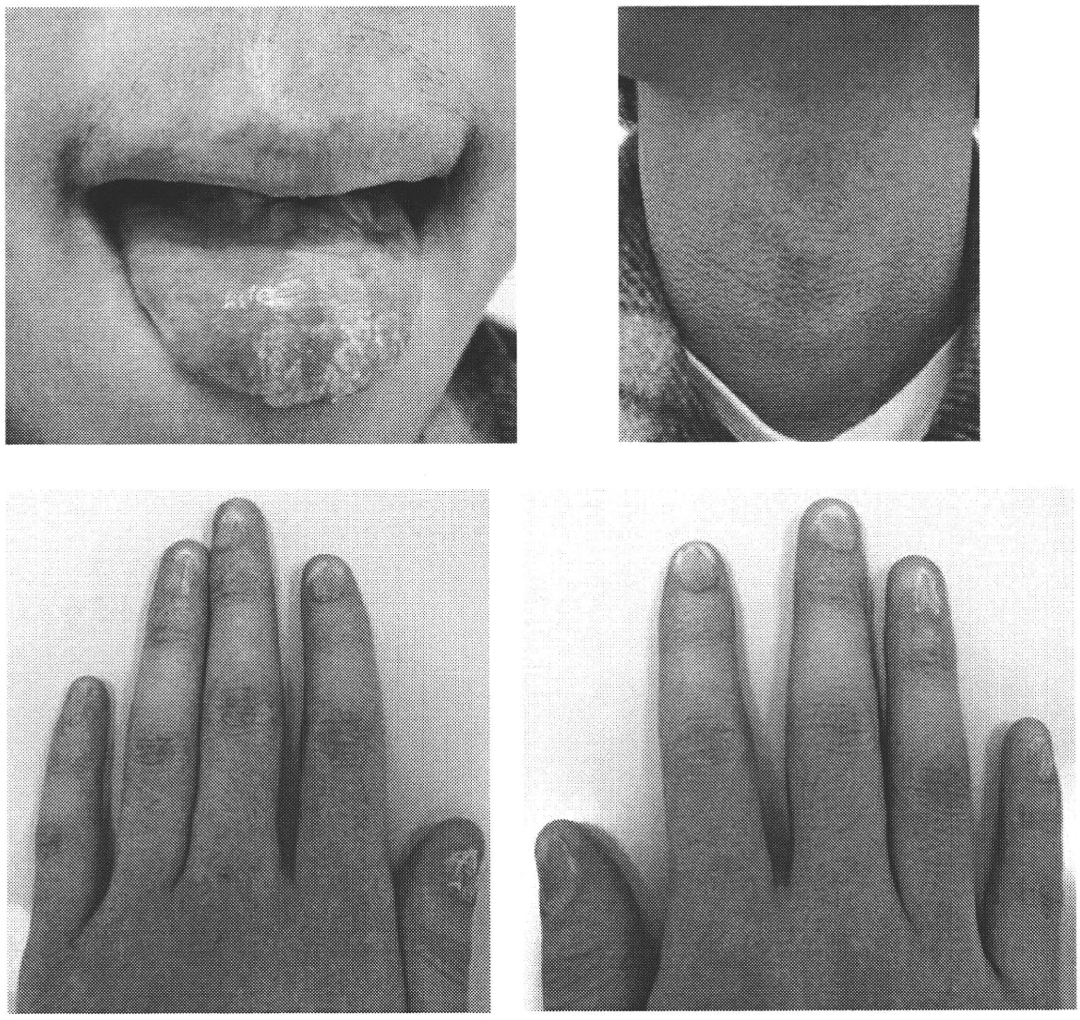

図 1 DKC の特徴的身体所見
左上：舌の粘膜白斑症，右上：皮膚の網状色素沈着，下：爪の萎縮

表 1 テロメア関連遺伝子変異と疾患

遺伝子(蛋白)	染色体存在部位	DKC における変異頻度	変異の type	疾 患
Telomerase				
TERC	3q21-28	5～10%	Heterozygous	AD-DKC, AA, ET, MDS, PNH, PF
TERT(TERT)	5p15.33	5%	Heterozygous Biallelic	AD-DKC, AA, HHS, PF AR-DKC, HHS
DKC1(Dyskerin)	Xq28	30%	Hemizygous	X-linked DKC, HHS
NHP2(NHP2)	5q35.3	1%	Biallelic	AR-DKC
NOP10(NOP10)	15q14-q15	1%	Homozygous	AR-DKC
Shelterin				
TINF2(TINF2)	14q11.2	10～15%	Heterozygous	AD-DKC, AA, HHS, RS

文献 7 より改変

AD-DKC: 常染色体優性遺伝型 DKC, AA: 再生不良性貧血，ET, 本態性血小板血症，MDS: 骨髄異形成症候群，PNH: 発作性夜間ヘモグロビン尿症，PF: 肺線維症，HHS: Hoyeraal-Hreidarsson syndrome, X-kinked DKC: X 連鎖劣性遺伝型 DKC, AR-DKC: 常染色体劣性遺伝型 DKC, RS: Revesz Syndrome

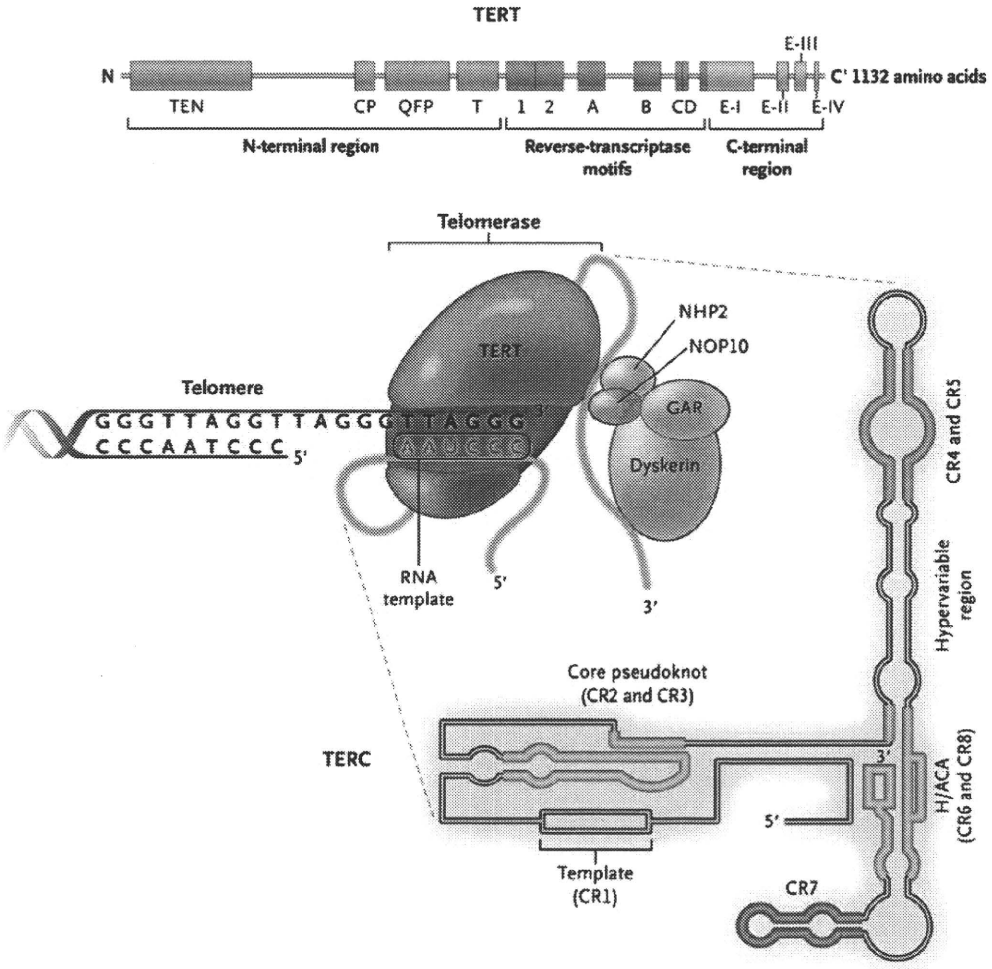

図 2 テロメラーゼ複合体
文献 9 より改変

亡する[11]。遺伝型式の大多数は X 連鎖劣性遺伝の男児とされてきたが，女児の HHS も報告されるようになった[11]。最近の報告では HHS の 1/3 の症例は女児で，その遺伝型式は常染色体劣性遺伝とされている[10]。HHS は独立した疾患として考えられていたが，その後 HHS に *DKC1* の T47M や S121 G などの変異が発見され DKC の重症型と考えられるようになった[11, 12]。

X 連鎖劣性遺伝型の DKC

DKC1 遺伝子（*DKC1*）は，染色体 Xq28 上にコードされ，X 連鎖劣性遺伝型の DKC の原因遺伝子である。*DKC1* によって翻訳される Dyskerin は核内蛋白の small nucleolar RNAs（snoRNA）のひとつで，boxH/ACA ドメインをもち他の snoRNA である NOP10, NHP2, GAR1 と複合体を形成し ribosomal RNA（rRNA）の processing や pre rRNA の転写産物の翻訳後修飾（pseudouridylation）に関与していると考えられている[13]。また Dyskerin を含む snoRNA 複合体は *TERC* の boxH/ACA ドメインと結合しテロメラーゼ複合体の processing と安定化の役割を果たしている（図 2）[13]。

X 連鎖型の DKC はこの *DKC1* の変異によって引き起こされると考えられているが，その変異の大多数は point mutation で large deletion やスプライス変異は稀である。これは *DKC1* の knockout マウスは胎性致死を起すことから，Dyskerin は細胞の生存に必須の蛋白であるためではないかと予想される[14]。*DKC1* の変異は exon 3, 4, 10, 11, 12 に集中しており，中でも exon 11 の PUA pseudouridin 合成酵素モチーフ上には多くの変異が認められる。特に *DKC1* 変異の約 30%に認められる A353 V は，hot spot と考えられており，*TERC* と snoRNA の accumulation，テロメラーゼ活性，rRNA processing や pseudouridylation に障害を与えて DKC の病態への関与が示されている[15]。また TruB pseudouridin 合成酵素モチーフの存在する領域の変異である S121

G や R158 W が DKC の重症型と考えられている HHS の表現型を示すことは興味深い点である[11]。しかし DKC と HH 両者に認められる変異も存在し，変異部位と DKC の重症度，HHS との関連には不明な点が多い[10,11]。さらに *DKC1* の promoter 領域には 3 つの GC-rich *cis*-elements が存在し Sp1 と Sp3 により *DKC1* の発現が調節されている。その Sp1 binding site の変異である-141C/G が *DKC1* の発現量を低下させ DKC を発症させることが報告されており，DKC は Dyskerin の変異による質的な異常だけでなく，量的な異常でも発症することが示唆されている[16]。

DKC のモデルとしては *DKC1* の exon 12-15 の欠損または exon 15 のみ欠損する Dyskerin hypomorphic 変異マウスでの解析が行われている[17]。この *DKC1* の発現を著しく低下させたモデルマウスでは最初の第 2 世代目までに DKC の表現型が再現される。興味深いことに，DKC の表現型が再現される第 2 世代目では，rRNA の processing や m*TERC* の発現とテロメラーゼ活性の低下は認められるが，テロメア長の短縮は認められず，第 4 世代目になってようやくテロメア長の短縮化が認められる[17]。このことは DKC の病態の形成にリボゾームの機能障害が関与していることを示している。

常染色体優性遺伝型の DKC

TERC と *TERT* 遺伝子変異

常染色体優性遺伝型の DKC の原因遺伝子としてはテロメラーゼ複合体の *TERC* と *TERT* が同定されている。*TERC* は染色体 3q21-28 上にコードされ，蛋白に翻訳されない 451bp の RNA としてテロメア伸展における鋳型の役割をしている[1,18]。*TERC* は自身で 2 次構造を形成し 5' 側の pseudoknot ドメインと CR4-CR5 ドメインは TERT と結合しテロメラーゼ活性に関与している[1,18]。一方 3' 側の boxH/ACA ドメインは Dyskerin などの snoRNA 蛋白と結合し，CR7 ドメインは small Cajalbody RNAs 蛋白（scaRNAs）と CAB box を介して結合することでテロメラーゼ複合体の processing や stability に関与している（図 2）[1,18]。scaRNAs 蛋白は核内の Cajalbody に存在し snoRNA と同様に rRNA に対しての pseudouridylation や methylation などの修飾する機能があると考えられている[19]。一方テロメラーゼ複合体において逆転写酵素の役割をもつ *TERT* は染色体 5p15 にコードされ *TERC* binding の機能がある N-terminus, 7 つの conserved motifs があり逆転写活性をもつ reverse transcriptase（RT）と telomerase multimerization の機能がある C-terminu の 3 つの region で構成されている（図 2）[1,18]。

常染色体優性遺伝型の DKC の特徴は，X 連鎖劣性遺伝型の DKC と比較して症状や検査所見の異常が軽度である症例が多いということである[6~8]。これは後述の不全型 DKC では *DKC1* 変異は認められず，その大多数において *TERC* や *TERT* の変異が認められることからも推測される[6~9]。*in vitro* の機能解析では，*TERC* の鋳型となる配列の変異は dominant negative 効果でテロメラーゼ活性を減弱させるが，その他の変異は haploinsufficiency 効果を示し，テロメラーゼ活性の減弱の程度は弱く，このことが常染色体優性遺伝型の DKC の症状や検査所見の異常が軽度である一つの理由として考えられている[20~22]。またモデルマウスでも同様の結果がえられていて，上述の *DKC1* 低発現マウスが第 2 世代目までに DKC の表現型が再現されるのに対して，*TERC* や *TERT* の knockout マウスでは 1 世代ごとにテロメアの短縮が認められ，世代が進むにつれて前者では精子形成の欠損，造血細胞の増殖障害などを，後者では消化管粘膜上皮のアポトーシスなどが認めるようになるが，DKC の表現型は示さない[6,8,23]。

しかし一方で *TERT* の変異を有する HHS の表現型を示す症例が存在しており，これらの遺伝子変異の部位や両アレルの変異の存在などが DKC の表現型に関与している可能性がある[24]。また *TERC* の変異が認められる DKC の家系においては世代が進むにつれて発症年齢が早まりテロメア長の短縮も顕著になってくる世代促進現象が認められる[25]。このことは上述のマウスモデルでも同様の結果が得られており，DKC の表現型には世代の促進が重要な役割をしていると予想される[17,23]。そして Fanconi 貧血などの他の遺伝性骨髄不全症の発症年齢中央値が 10 歳以下なのに対して，DKC は 15 歳前後で，半数近くの症例が成人になって診断されていることから，世代促進だけでなく加齢も DKC の表現型に重要な役割をしていると予想される（図 3）[26]。

TINF2 遺伝子変異

近年染色体 14q11.2 上に存在する *TINF2* の変異が常染色体優性遺伝型の DKC で同定された[27,28]。*TINF2* は Shelterin 複合体を構成する TIN2 をコードしている[29]。テロメア DNA の最末端部位は，DNA の 3' 末端が突出（オーバーハング）して一本鎖になっている。また哺乳類のテロメアはおり曲がって T ループと呼ばれる構造をとり，このオーバーハングした一本鎖 DNA は，その上流のテロメア二本鎖の中に入り込み D ループを構成する[29]。Shelterin 複合体はこの特異的な構造形成や保護などを行っているが，Shelterin 複合体は，二本鎖 DNA と結合する TRF1 と TRF2，一本鎖 DNA に結合する POT1，これらの蛋白を結合させ複合体を形成する役割をもつ TIN2，RAP1，TPP1 で構成されている（図 4）[29]。

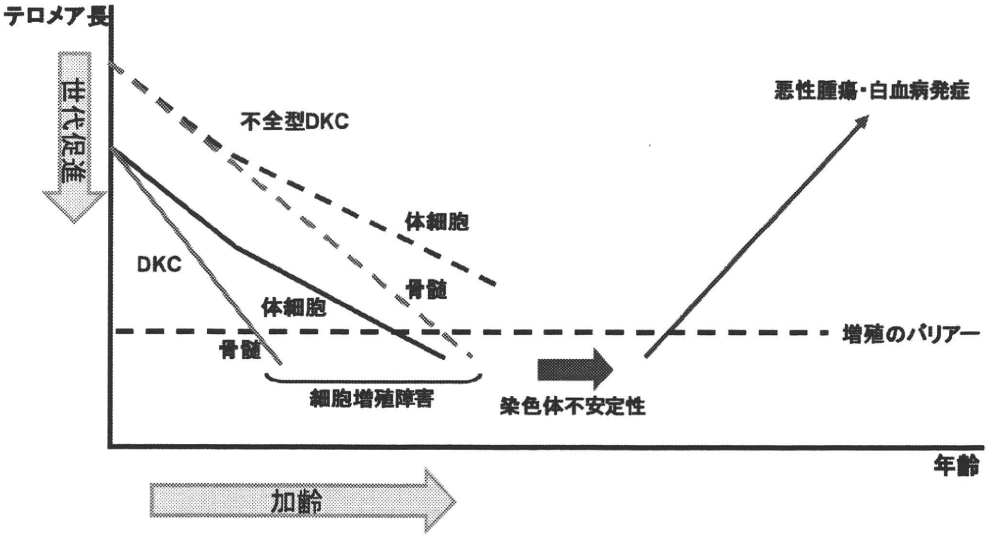

図3 DKCの発症機序
DKCはテロメア関連遺伝子変異によるテロメア伸長補正の障害，世代促進，加齢が病態の形成には重要である。

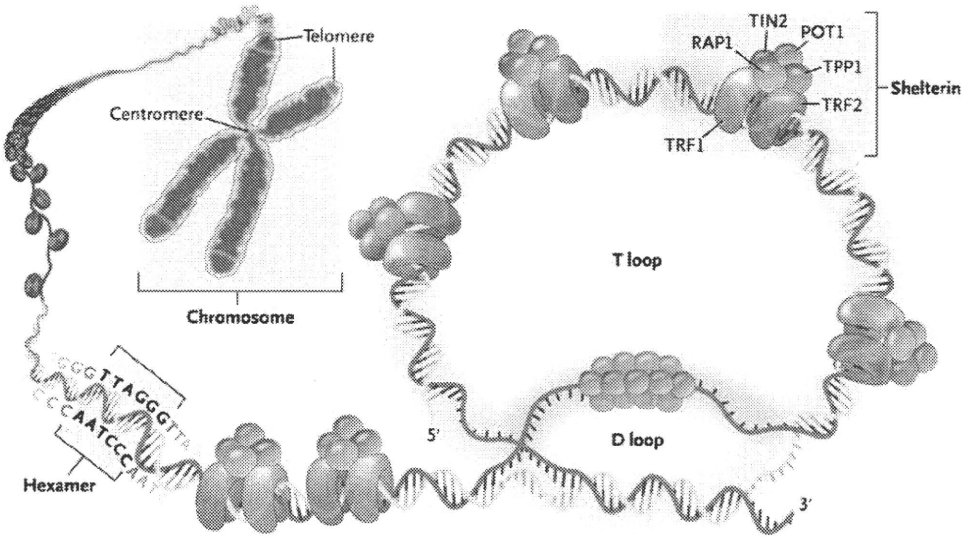

図4 Shelterin複合体
文献9より改変

*TINF2*の変異はDKCの約10～15%に認められ，DKC1の次に多く認められる遺伝子変異である[7]。*TINF2*の変異の多くはヘテロのpoint mutationで，半数以上がTRF1との結合ドメインの中のコドン282arginineの変異である。またその他の変異の大多数もコドン282近傍の変異であり，この領域が*TINF2*の機能として重要であることを示唆している。*TINF2*の変異の機能に関しては不明な点が多いいが，*TINF2*のknock outマウスは胎性致死となることから，*TINF2*は細胞の生存に必修の蛋白であることが予想される[30]。また*TINF2*のconservation regionの変異は，TRF1との結合が出来なくなることでShelterin複合体の機能が障害されるのではないかと予想されている[31]。

常染色体劣性型のDKC

常染色体劣性遺伝型のDKCの頻度は少なく，全体の1～2%にしか認められない[7]。これまでに原因遺伝子としては上述の*TERT*や上述のsnoRNAである*NOP10*, *NHP2*が同定されている（表1）[7, 13]。常染色体劣性遺伝型のDKCに認められた*TERT*の変異は，RTドメイン

の中に位置するR811CとR901Wのホモ変異である[24]。これらの変異の機能はhaploinsufficiency効果でテロメラーゼ活性を減弱させるが，ホモ変異であるためテロメラーゼ活性の減弱が強くDKCやHHSの表現型を示す。しかしこれらの*TERT*変異のDKC発症形式が常染色体劣性遺伝型かは不明瞭で，R811C症例のヘテロの変異を有する両親は軽度ではあるがDKCの表現型とも考えられる症候を有しており，世代促進が進んでいないためにDKCの表現型が出ていないだけかもしれない。

NOP10やNHP2は，Dyskerinなどと snoRNA複合体を形成し，*TERC*のboxH/ACAドメインと結合しテロメラーゼ複合体のprocessingと安定化の役割を果たしている（図2）[13, 19]。これまでに*NOP10*はホモ変異が，*NHP2*はホモ変異と両アレル変異が認めているが，これらの変異によって*TERC*の発現の減少し，テロメラーゼ活性が減弱することでDKCが発症すると考えられている[32, 33]。

不全型のDKC

成人になって特徴的身体所見を伴わず緩徐に発症する不全型のDKCの存在が明らかになった[34]。不全型のDKCは，臨床的には再生不良性貧血や骨髄異形成症候群（MDS）などと診断されていることが多く[35, 36]，本邦においても再生不良性貧血や骨髄異形成症候群の不応性貧血などの骨髄不全症の2～5%に不全型のDKCが認められる（表2）[37~39]。不全型のDKCの原因遺伝子としては，*TERC*，*TERT*，*TINF2*の報告があるが（表1），上述の様に*TERC*，*TERT*の変異はhaploinsufficiency効果を示し，テロメラーゼ活性の減弱の程度は弱いため，DKCの表現型となるには，世代促進や加齢が必要となることがある。こうした変異の場合は，世代の早い症例ではDKCの表現型が軽度で，不全型DKCとして診断されるのではないかと予想する。

これまで再生不良性貧血の約1/3の症例はテロメア長が短縮し，再生不良性貧血の重症度，免疫抑制療法への不応性との関連が示唆されていたが[40~42]，これらは不全型DKCの存在が明らかになる以前の検討で，テロメア長の短縮化が再生不良性貧血の病態にどの様に関与しているかは明らかではない。しかし不全型のDKCは，効果の得られない免疫抑制療法が行われたり，血縁間同種造血幹細胞移植の際に健常人と区別がつきづらい軽症の不全型DKCである同胞がドナーと選ばれたりすることがあるため，臨床的に診断を明確にすることは大変重要である[34~39]。こうした不全型のDKCをスクリーニングするのに，骨髄不全症の診断時にテロメア長の測定をすることは有用であると考える。

DKCの治療

現在のところDKCの根本的治療は開発されていない。DKCの主な死因は造血障害に伴う様々な合併症と晩期の悪性腫瘍によるものが大多数である[7, 11]。これまで前者に対しては造血幹細胞移植（stem cell transplantation: SCT）が試みられてきたが，通常の骨髄破壊的前処置によるSCTは，移植後の肺線維症などの肺合併症，消化管狭窄，肝中心静脈閉塞症などの治療関連毒性が強く，長期生存例は稀であった[43]。DKCにおいてSCTの治療関連毒性が強い理由は，皮膚，消化管，肺胞上皮などの幹細胞のテロメア伸長補正の障害による増殖障害があるためと予想されている[43]。その後fludarabineをベースとした骨髄非破壊的前処置によるSCTでは，上述の治療関連毒性が軽減され長期の生存例も認められるようになった[43~45]。しかし上述のようにDKCはHHSから不全型のDKCまでその表現型は様々で，どのような症例に対してどの時期にどのようにしてSCTを行うかといった臨床的な適応は明らかになっていない。また他の後天的な骨髄不全症に対するSCTに比べてDKCに対してのSCTは，晩期の悪性腫瘍の合併がより高率となる可能性もあり今後の症例の蓄積が必要である。

DKCの骨髄不全症に対しての保存的治療として以前よりanabolic steroidやG-CSFなどの有効性が報告され

表2 本邦で認められた不全型のDKC

遺伝子	変異部位	年齢	性	臨床診断	家族歴	染色体	テロメア短縮化	治 療
TERC	n323 C/T	72	男性	MDS RA	(−)	46XY	ND	metenoloneにて軽快
	G280K	3	男性	sAA	(−)	46XY	(+)	免疫抑制治療に反応なし
TERT	G682D	10	男性	mAA	(−)	ND	ND	不明
	T726M	9	女性	sAA	(−)	ND	(+)	免疫抑制治療に反応なし
	R282C	22	男性	sAA	(−)	46XY	(+)	免疫抑制治療に反応なし
TINF2	n865-866 deletion	29	男性	sAA	(−)	46XY	(+)	免疫抑制治療に反応なし

文献37～39より

MDS: 骨髄異形成症候群，sAA: 重症再生不良性貧血，mAA: 中等症再生不良性貧血，ND: 検査未施行。

てきた[7, 46, 47]。特に anabolic steroid である oxymetholone（0.5～5 mg/kg/day）の治療によって約 2/3 の症例で血液学的な何らかの有効性が認められたとされている。これまで anabolic steroid による DKC の血液学的な改善の機序は不明であったが，近年 *TERT* の promoter 領域にエストロゲン結合領域が認められ，アンドロゲンやエストロゲンなどの性ホルモンがテロメラーゼ活性を亢進させることが示された[48]。このことから成人以降で診断された不全型の DKC に対しても anabolic steroid などによる治療は有効であると思われる。

おわりに

DKC は，X 連鎖劣性遺伝型の古典的な DKC が発見され，その原因がテロメアの機能不全であることが明らかになり，その後テロメアの機能不全という観点より不全型の DKC の存在が明らかになってきた。しかし依然として確立した治療法はなく，さらなる病態の解析による新たな治療法の確立が期待される。最近になり再プログラム化された DKC 由来の induced pluripotent stem (iPS) 細胞において，OCT4 や NANOG といった分化増殖万能性の維持に必修の転写因子が，*TERC* や *DKC1* の発現を亢進させ，DKC 由来のテロメラーゼ複合体の機能障害を克服し，テロメアの再伸長が認められることが報告された[49]。このことは，DKC 由来の iPS 細胞は，テロメア関連遺伝子変異によるテロメア伸長の機能障害があっても，テロメア伸長が回復することを示しており，将来の治療法の開発に発展するものと期待される。

文 献

1) O'Sullivan RJ, Karlseder J. Telomeres: protecting chromosomes against genome instability. Nat Rev Mol Cell Biol. 2010; **11**: 171-181.
2) Harley CB, Futcher AB, Greider CW. Telomeres shorten during ageing of human fibroblasts. Nature. 1990; **345**: 458-460.
3) Harley CB, Vaziri H, Counter CM, Allsopp RC. The telomere hypothesis of cellular aging. Exp Gerontol. 1992; **27**: 375-382.
4) Watson JD. Origin of concatemeric T7 DNA. Nat New Biol. 1972; **239**: 197-201.
5) Olovnikov AM. A theory of marginotomy. The incomplete copying of template margin in enzymic synthesis of polynucleotides and biological significance of the phenomenon. J Theor Biol. 1973; **41**: 181-190.
6) Calado RT, Young NS. Telomere maintenance and human bone marrow failure. Blood. 2008; **111**: 4446-4455.
7) Walne AJ, Dokal I. Advances in the understanding of dyskeratosis congenita. Br J Haematol. 2009; **145**: 164-172.
8) Carroll KA, Ly H. Telomere dysfunction in human diseases: the long and short of it! Int J Clin Exp Pathol. 2009; **2**: 528-543.
9) Calado RT, Young NS. Telomere diseases. N Engl J Med. 2009; **361**: 2353-2365.
10) Vulliamy TJ, Marrone A, Knight SW, Mason PJ, Dokal I. Mutations in dyskeratosis congenita: their impact on telomere length and the diversity of clinical presentation. Blood. 2006; **107**: 2680-2685.
11) Dokal I. Dyskeratosis congenita in all its forms. Br J Haematol. 2000; **110**: 768-779.
12) Marrone A, Dokal I. Dyskeratosis congenita: molecular insights into telomerase function, ageing and cancer. Expert Rev Mol Med. 2004; **6**: 1-23.
13) Filipowicz W, Pogacić V. Biogenesis of small nucleolar ribonucleoproteins. Curr Opin Cell Biol. 2002; **14**: 319-327.
14) He J, Navarrete S, Jasinski M, et al. Targeted disruption of Dkc1, the gene mutated in X-linked dyskeratosis congenita, causes embryonic lethality in mice. Oncogene. 2002; **21**: 7740-7744.
15) Mochizuki Y, He J, Kulkarni S, Bessler M, Mason PJ. Mouse dyskerin mutations affect accumulation of telomerase RNA and small nucleolar RNA, telomerase activity, and ribosomal RNA processing. Proc Natl Acad Sci U S A. 2004; **101**: 10756-10761.
16) Salowsky R, Heiss NS, Benner A, Wittig R, Poustka A. Basal transcription activity of the dyskeratosis congenita gene is mediated by Sp1 and Sp3 and a patient mutation in a Sp1 binding site is associated with decreased promoter activity. Gene. 2002; **293**: 9-19.
17) Ruggero D, Grisendi S, Piazza F, et al. Dyskeratosis congenita and cancer in mice deficient in ribosomal RNA modification. Science. 2003; **299**: 259-262.
18) Cong YS, Wright WE, Shay JW. Human telomerase and its regulation. Microbiol Mol Biol Rev. 2002 ; **66**: 407-425.
19) Chen JL, Greider CW. Telomerase RNA structure and function: implications for dyskeratosis congenita. Trends Biochem Sci. 2004; **29**: 183-192.
20) Xin ZT, Beauchamp AD, Calado RT, et al. Functional characterization of natural telomerase mutations found in patients with hematologic disorders. Blood. 2007; **109**: 524-532.
21) Marrone A, Stevens D, Vulliamy T, Dokal I, Mason PJ. Heterozygous telomerase RNA mutations found in dyskeratosis congenita and aplastic anemia reduce telomerase activity via haploinsufficiency. Blood. 2004; **104**: 3936-3942.
22) Ly H, Calado RT, Allard P, et al. Functional characterization of telomerase RNA variants found in patients with hematologic disorders. Blood. 2005; **105**: 2332-2339.
23) Cheong C, Hong KU, Lee HW. Mouse models for telomere and telomerase biology. Exp Mol Med. 2003; **35**: 141-153.
24) Marrone A, Walne A, Tamary H, et al. Telomerase reverse-transcriptase homozygous mutations in autosomal recessive dyskeratosis congenita and Hoyeraal-Hreidarsson syndrome.

Blood. 2007; **110**: 4198-4205.
25) Vulliamy T, Marrone A, Szydlo R, Walne A, Mason PJ, Dokal I. Disease anticipation is associated with progressive telomere shortening in families with dyskeratosis congenita due to mutations in TERC. Nat Genet. 2004; **36**: 447-449.
26) Alter BP. Diagnosis, genetics, and management of inherited bone marrow failure syndromes. Hematology Am Soc Hematol Educ Program. 2007; 29-39.
27) Savage SA, Giri N, Baerlocher GM, Orr N, Lansdorp PM, Alter BP. TINF2, a component of the shelterin telomere protection complex, is mutated in dyskeratosis congenita. Am J Hum Genet. 2008; **82**: 501-509.
28) Walne AJ, Vulliamy T, Beswick R, Kirwan M, Dokal I. TINF2 mutations result in very short telomeres: analysis of a large cohort of patients with dyskeratosis congenita and related bone marrow failure syndromes. Blood. 2008; **112**: 3594-3600.
29) de Lange T. Shelterin: the protein complex that shapes and safeguards human telomeres. Genes Dev. 2005; **19**: 2100-2110.
30) Chiang YJ, Kim SH, Tessarollo L, Campisi J, Hodes RJ. Telomere-associated protein TIN2 is essential for early embryonic development through a telomerase-independent pathway. Mol Cell Biol. 2004; **24**: 6631-6634.
31) Kim SH, Davalos AR, Heo SJ, et al. Telomere dysfunction and cell survival: roles for distinct TIN2-containing complexes. J Cell Biol. 2008; **181**: 447-460.
32) Walne AJ, Vulliamy T, Marrone A, et al. Genetic heterogeneity in autosomal recessive dyskeratosis congenita with one subtype due to mutations in the telomerase-associated protein NOP10. Hum Mol Genet. 2007; **16**: 1619-1629.
33) Vulliamy T, Beswick R, Kirwan M, et al. Mutations in the telomerase component NHP2 cause the premature ageing syndrome dyskeratosis congenita. Proc Natl Acad Sci U S A. 2008; **105**: 8073-8078.
34) Fogarty PF, Yamaguchi H, Wiestner A, et al. Late presentation of dyskeratosis congenita as apparently acquired aplastic anaemia due to mutations in telomerase RNA. Lancet. 2003; **362**: 1628-1630.
35) Yamaguchi H, Baerlocher GM, Lansdorp PM, et al. Mutations of the human telomerase RNA gene (TERC) in aplastic anemia and myelodysplastic syndrome. Blood. 2003; **102**: 916-918.
36) Yamaguchi H, Calado RT, Ly H, et al. Mutations in TERT, the gene for telomerase reverse transcriptase, in aplastic anemia. N Engl J Med. 2005; **352**: 1413-1424.
37) Liang J, Yagasaki H, Kamachi Y, et al. Mutations in telomerase catalytic protein in Japanese children with aplastic anemia. Haematologica. 2006; **91**: 656-658.
38) Takeuchi J, Ly H, Yamaguchi H, et al. Identification and functional characterization of novel telomerase variant alleles in Japanese patients with bone-marrow failure syndromes. Blood Cells Mol Dis. 2008; **40**: 185-191.
39) Yamaguchi H, Inokuchi K, Takeuchi J, et al. Identification of TINF2 gene mutations in adult Japanese patients with acquired bone marrow failure syndromes. Br J Haematol. In press.
40) Ball SE, Gibson FM, Rizzo S, et al. Progressive telomere shortening in aplastic anemia. Blood. 1998; **91**: 3582-3592.
41) Brümmendorf TH, Maciejewski JP, Mak J, Young NS, Lansdorp PM. Telomere length in leukocyte subpopulations of patients with aplastic anemia. Blood. 2001; **97**: 895-900.
42) Lee JJ, Kook H, Chung IJ, et al. Telomere length changes in patients with aplastic anaemia. Br J Haematol. 2001; **112**: 1025-1030.
43) Ostronoff F, Ostronoff M, Calixto R, et al. Fludarabine, cyclophosphamide, and antithymocyte globulin for a patient with dyskeratosis congenita and severe bone marrow failure. Biol Blood Marrow Transplant. 2007; **13**: 366-368.
44) de la Fuente J, Dokal I. Dyskeratosis congenita: advances in the understanding of the telomerase defect and the role of stem cell transplantation. Pediatr Transplant. 2007; **11**: 584-594.
45) Coman D, Herbert A, McGill J, Lockwood L, Hallahan A. Unrelated cord blood transplantation in a girl with Hoyeraal-Hreidarsson syndrome. Bone Marrow Transplant. 2008; **42**: 293-294.
46) Bayne S, Liu JP. Hormones and growth factors regulate telomerase activity in ageing and cancer. Mol Cell Endocrinol. 2005; **240**: 11-22.
47) Erduran E, Hacisalihoglu S, Ozoran Y. Treatment of dyskeratosis congenita with granulocyte-macrophage colony-stimulating factor and erythropoietin. J Pediatr Hematol Oncol. 2003; **25**: 333-335.
48) Calado RT, Yewdell WT, Wilkerson KL, et al. Sex hormones, acting on the TERT gene, increase telomerase activity in human primary hematopoietic cells. Blood. 2009; **114**: 2236-2243.
49) Agarwal S, Loh YH, McLoughlin EM, et al. Telomere elongation in induced pluripotent stem cells from dyskeratosis congenita patients. Nature. 2010; **464**: 292-296.

Endothelial–Mesenchymal Transition in Bleomycin-Induced Pulmonary Fibrosis

Naozumi Hashimoto[1], Sem H. Phan[2], Kazuyoshi Imaizumi[1], Masaki Matsuo[1], Harunori Nakashima[1], Tsutomu Kawabe[3], Kaoru Shimokata[4], and Yoshinori Hasegawa[1]

[1]Department of Respiratory Medicine, Nagoya University Graduate School of Medicine, Nagoya, Japan; [2]Department of Pathology, University of Michigan, Ann Arbor, Michigan; [3]Department of Medical Technology, Nagoya University Graduate School of Health Science, Nagoya, Japan; and [4]College of Life and Health Sciences, Department of Biomedical Sciences, Chubu University, Kasugai, Japan

The pathological hallmark lesions in idiopathic pulmonary fibrosis are the fibroblastic foci, in which fibroblasts are thought to be involved in the tissue remodeling, matrix deposition, and cross-talk with alveolar epithelium. Recent evidence indicates that some fibroblasts in fibrosis may be derived from bone marrow progenitors as well as from epithelial cells through epithelial–mesenchymal transition. To evaluate whether endothelial cells could represent an additional source for fibroblasts, bleomycin-induced lung fibrosis was established in Tie2-Cre/CAG-CAT-LacZ double-transgenic mice, in which LacZ was stably expressed in pan-endothelial cells. Combined X-gal staining and immunocytochemical staining for type I collagen and α-smooth muscle actin revealed the presence of X-gal–positive cells in lung fibroblast cultures from bleomycin-treated mice. To explore the underlying mechanisms, by which loss of endothelial-specific markers and gain of mesenchymal phenotypes could be involved in microvascular endothelial cells, the effects of activated Ras and TGF-β on the microvascular endothelial cell line MS1 were analyzed. Combined treatment with activated Ras and TGF-β caused a significant loss of endothelial-specific markers, while inducing *de novo* mesenchymal phenotypes. The altered expression of these markers in MS1 cells with activated Ras persisted after withdrawal of TGF-β *in vitro* and *in vivo*. These findings are the first to show that lung capillary endothelial cells could give rise to significant numbers of fibroblasts through an endothelial–mesenchymal transition in bleomycin-induced lung fibrosis model.

Keywords: fibroblasts; myofibroblasts; endothelial cells; LacZ; fibrosis

CLINICAL RELEVANCE

This study is the first to show that lung endothelial cells could give rise to significant numbers of fibroblasts in lung fibrosis model. The underlying mechanism might be suggested by the findings that combined treatment with activated Ras and TGF-β could cause endothelial–mesenchymal transition in endothelial cells.

Idiopathic pulmonary fibrosis (IPF) is a devastating disease without effective therapy (1). The hallmark lesions are the fibroblastic foci representing focal areas of active fibrogenesis featuring vigorous fibroblast replication and exuberant extracellular matrix deposition, which may lead to obliteration of the distal air space. Fibroblasts represent the key source of interstitial collagens, but fibroblasts isolated from IPF lungs have heterogenous phenotypes and properties different from that of normal lung fibroblasts (2). While it has been assumed that they arise only from intrapulmonary mesenchymal cells, one potential explanation for this heterogeneity is that fibroblasts may be derived from multiple cell origins under pathological conditions such as IPF. Recent mounting evidence suggests that bone marrow (BM)-derived fibroblasts may be recruited to various injured tissue sites and play an important role in the establishment of fibrosis at those sites (3, 4). Another potential explanation for their heterogeneity is the possible emergence during pulmonary fibrosis of alveolar epithelial cells (AECs)-derived fibroblasts through epithelial–mesenchymal transition (epithelial-MT) (5, 6).

Epithelial-MT, in which persistent loss of epithelial markers and *de novo* expression of mesenchymal markers are involved, is assumed to have a critical role in not only tissue development during embryogenesis but also pathological condition (7, 8). One central feature of epithelial-MT is the co-operation of TGF-β signaling with receptor tyrosine kinase (RTK) signaling, which activates Ras/ERK/MAPK pathway, resulting in the establishment of epithelial-MT, not "scattering", in which the phenotype changes are fully reversible after removal of scattering-inducing factor, such as fibroblast growth factor (FGF), hepatocyte growth factor (HGF), or TGF-β alone (7).

Endothelial cells in the lung vasculature represent one of main cellular components of structural cells in the lung (9). In animal models of various lung diseases, they have been shown to function not only as a mere barrier between the blood compartment and the interstitial and air spaces, but also be involved in new vessel formation (10). Although a few *in vitro* studies reported the possibility of endothelial cells as a source of α-smooth muscle actin (α-SMA)–expressing mesenchymal cells or that of type I collagen (Col I)–producing cells (11, 12), it has not fully been determined whether endothelial cells could give rise to another population of fibroblasts under certain pathological conditions such as lung fibrosis.

These previous findings led us to investigate whether lung capillary endothelial cells could represent an additional source of fibroblasts, possibly through endothelial–mesenchymal transition (endothelial-MT), in an experimental lung fibrosis model, and if so, to elucidate the underlying mechanism, that is, whether combined signaling with activated Ras and TGF-β could induce endothelial-MT.

We generated Tie2-Cre/CAG-CAT-LacZ double-transgenic mice (CAG mice), in which *de novo* LacZ expression will stably label the Tie2 promoter-activated cells after Cre-mediated

(Received in original form January 22, 2009 and in final form August 28, 2009)

This work was supported by Nagao Memorial Fund, Grant-in-Aid for Young Scientists (B) (17790530), Grant-in-Aid for Scientific Research (C) (19590890), and the 21st Century COE Program "Integrated Molecular Medicine for Neuronal and Neoplastic Disorders" of the Ministry of Education, Culture, Sports, Science and Technology. Support from National Institutes of Health grants HL28737 and HL52285 (to S.H.P.) is also acknowledged.

Correspondence and requests for reprints should be addressed to Yoshinori Hasegawa, M.D., Department of Respiratory Medicine, Nagoya University Graduate School of Medicine, 65 Tsurumai-cho, Showa-ku, Nagoya 466-8550 Japan. E-mail: yhasega@med.nagoya-u.ac.jp

This article has an online supplement, which is accessible from this issue's table of contents at www.atsjournals.org

Am J Respir Cell Mol Biol Vol 43. pp 161–172, 2010
Originally Published in Press as DOI: 10.1165/rcmb.2009-0031OC on September 18, 2009
Internet address: www.atsjournals.org

recombination. *In vivo* studies using the bleomycin (BLM)-induced lung fibrosis model with these mice successfully demonstrated that lung capillary endothelial cells could represent another potential source of fibroblasts/myofibroblasts, possibly through an endothelial-MT. The results of the study *in vitro* showed that combined treatment with activated Ras and TGF-β could induce endothelial-MT in microvascular endothelial cells.

MATERIALS AND METHODS

Mice and Mouse Fibrosis Model

To obtain CAG mice, Tie2-Cre Tg mice were bred with CAG-CAT-LacZ Tg mice (13). Pulmonary fibrosis was induced by endotracheal BLM injection as before (4). All animal studies were reviewed and approved by the University Committee on Use and Care of Animals at Nagoya Graduate School of Medicine.

Collection of Lung Samples and Lung Fibroblasts from BLM-Treated Mice

At Day 28 after BLM injection, both lungs from treated mice were lavaged with PBS and then frozen in OCT compound (Miles, Elkhart, IN). Mouse lung fibroblasts were also isolated from lung tissues at Day 28 as before (14).

X-Gal Staining

For detection of β-galactosidase activity, cultured cells and lung tissues were incubated in an X-gal solution at 37°C overnight. Nuclei were stained with Hoechst 33342 for cultured fibroblasts or hematoxylin for lung tissues, respectively.

Cell Treatments and Analysis of Phenotype Changes *In Vitro*

The mouse microvascular endothelial cell line MS1 and activated Ras transduced MS1 (SVR) were maintained as before (15). After TGF-β treatment at 10 ng/ml for 24 hours, MS1 and SVR were harvested for assessment of targeted genes by real-time PCR, or endothelial-specific markers expression by FACS. For immunocytochemical determination of α-SMA, cultured cells in an 8-well Lab-Tek (Nalge Nunc International, Naperville, IL) Chamber Slide were also treated with 10 ng/ml TGF-β for 24 hours. To distinguish endothelial-MT *in vitro* from "scattering," these cells were cultured for another 24 hours after TGF-β removal, followed by phenotype analysis. To evaluate whether the cells can retain the phenotype changes, SVR were also re-plated into the new culture dish after TGF-β treatment and then analyzed as above.

In Vitro Analysis of Phenotype Alteration in Endothelial Cell Line by FACS

After treatment, the harvested cells were stained with appropriate dilutions of biotin-conjugated rat anti-mouse CD31 antibody, PE-conjugated rat anti-mouse CD34 antibody, biotin-conjugated rat anti-mouse Tie2 antibody, purified rat anti-mouse VE-cadherin antibody, or the appropriate isotype-matched controls, and then detected by subsequent staining with SAv-Cy-chrome for CD 31 and Tie2, and SAv-488-conjugated anti rat antibody for VE-cadherin, respectively. Dead cells were excluded from flow cytometry analysis by appropriate gating (4), and a total of 2×10^4 living cells were collected for each analysis on a FACSCalibur flow cytometer (BD Biosciences, San Jose, CA). The results are presented as overlaid histograms and the relative mean fluorescence intensity (MFI). The relative MFI was calculated by dividing the MFI units of CD31, CD34, Tie2, or VE-cadherin staining by the MFI units of isotype control staining in each sample (16).

Endothelial Cell Line Transplantation *In Vivo* and Isolation of Activated Ras-Transduced Endothelial Cells *Ex Vivo*

A million MS1 or SVR cells were inoculated subcutaneously into the flank of nude mice (17). At Day 28 after inoculation, *ex vivo* SVR cells from the resulting nodule were isolated as before (14). To eliminate host-derived cells such as fibroblasts, cultured cells were selected with neomycin. Isolated *ex vivo* SVR cells were treated with 10 ng/ml TGF-β and then harvested for the analysis as above. To evaluate lung metastasis in treated mice, H&E staining was performed for the lungs resected at Day 28.

Immunofluorescent Staining

Immunofluorescent stainings were performed for the collected samples as before (18). The slides were incubated with appropriate dilutions of primary antibodies, and then visualized by fluorescent reagents.

PCR Analysis for Expression of Targeted Genes

Real-time PCR was performed using a TaqMan ABI 7300 Sequence Detection System (PE Applied Biosystems, Foster City, CA). Fibronectin, Col I, Snail, and Twist mRNA were detected, using mixture reagents from TaqMan Gene Expression Assays (Applied Biosystems, Foster City, CA). The mRNA levels were normalized to glyceraldehyde-3-phosphate dehydrogenase (GAPDH) mRNA signal using TaqMan rodent GAPDH control reagents from Applied Biosystems (19). RT-PCR analysis for mRNA of TGFβR I (GenBank accession no. NM_009370) and II (GenBank accession no. NM_009371 for variant1 and NM_029575 for variant2), and GAPDH was performed with platinum Taq.

Statistical Analysis

The results were analyzed using the Mann-Whitney test for comparison between any two groups, and by nonparametric equivalents of ANOVA for multiple comparisons. $P < 0.05$ was considered to indicate statistical significance.

RESULTS

Generation of CAG Mice and Endothelial-MT in BLM-Induced Pulmonary Fibrosis

We investigated whether endogenous endothelial cells could represent a significant source of lung fibroblasts in an animal model of pulmonary fibrosis *in vivo*. To enable the tracking of fibroblasts derived from endothelial cell lineage *in vivo*, CAG mice were generated so that *de novo* irreversible LacZ expression by Tie2 promoter/enhancer–driven Cre-mediated recombination could be used as a marker for cells of endothelial cell origin (Figure 1A). As the primers used for amplification of CAG, designed on CAG promoter and the LacZ gene, can detect only the recombined allele of the CAG-CAT-LacZ target gene (13), the results of genotyping analysis revealed that the CAG mice carrying both Tie2-Cre gene and CAG-CAT-LacZ gene could express the *de novo* CAG promoter driven LacZ gene after Tie2 promoter/enhancer–driven Cre-mediated excision of the *loxP*-flanked chloramphenicol acetyltransferase (CAT) gene located between the CAG promoter and the *LacZ* gene, while littermates carrying either the Tie2-Cre or CAG-CAT-LacZ gene alone could not (Figure 1A). To evaluate the distribution of the cells with β-galactosidase activity in the lungs, X-gal staining was performed for the lung tissues from saline- or BLM-treated CAG mice at Day 28. Lungs from saline-treated CAG mice showed essentially normal lung architecture with expected blue staining of capillary endothelial cells (Figure 1B). Morphological evaluation for lungs from BLM-treated CAG mice revealed severe pulmonary fibrosis, characterized by loss of normal alveolar architecture, prominent disorganized thickening of the alveolar septa, and collapse of the alveolar space with organizing inflammatory infiltrate and fibroblasts (Figure 1C). These histological changes of lungs from BLM-treated CAG mice were comparable to those in BLM-treated wild type B6 mice (data not shown). In cellular fibrotic areas, large numbers of X-gal–positive cells were evident (Figure 1C), indicating that significant numbers of the cells in active fibrotic lesions were of endothelial origin. To further evaluate the distribution of these cells in fibrotic lungs of BLM-treated CAG mice, double immunofluorescent stain-

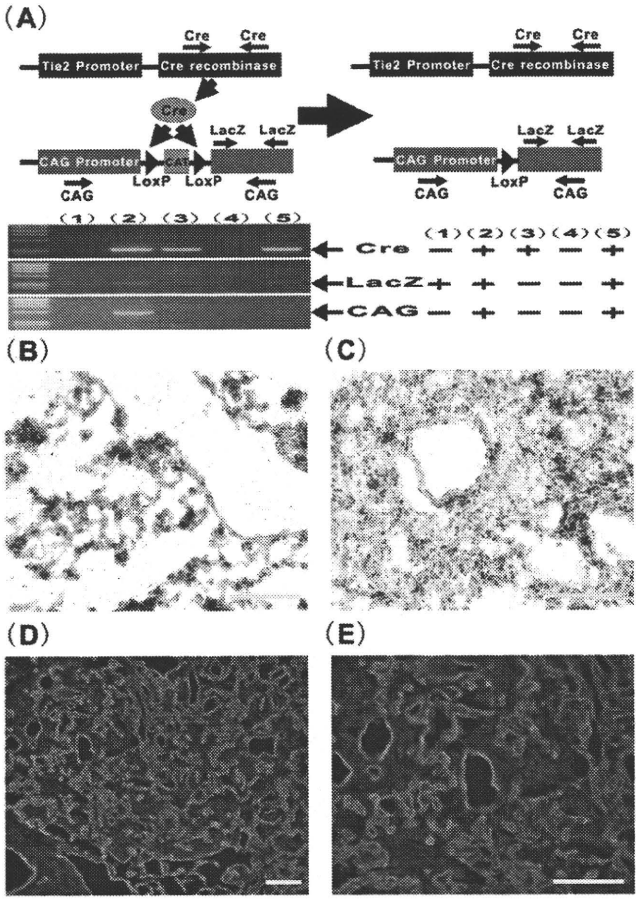

Figure 1. Generation of Tie2-Cre/CAG-CAT-LacZ double-transgenic mice (CAG mice) and bleomycin (BLM)-induced lung fibrosis model. To obtain CAG mice, Tie2-Cre Tg mice were bred with CAG-CAT-LacZ Tg mice. (*A*) *Top*: Schematic description of gene constructs in CAG mice. *Bottom*: Genotyping analyses. Genotyping analyses were performed for off spring of CAG mice. The representative electropherogram of Cre (*left top*), LacZ (*left middle*), and CAG (*left bottom*) were shown for a set of five offsprings. The results were summarized (*right panel*). X-gal staining was performed for the lung tissues from (*B*) saline- or (C) BLM- treated CAG mice at Day 28 (×400 magnification). Double immunostaining for CD31 (*green*) and Col I (*red*) was performed for the lung tissues from BLM mice (*D*, ×200 magnification; E, ×400 magnification). *Scale bars* in *B–D* indicate 50 μm.

ing for CD31 (Figure 1D and 1E, *green*), a representative endothelial maker, and Col I (Figure 1D and 1E, *red*), a marker for fibroblasts, was performed (Figures 1D and 1E, and Figures E1E and E1F in the online supplement). Although the immunostaining for the lungs of saline-treated CAG mice exhibited that Col I expression was observed either in CD31-expressing endothelial cells or in accordance with alveolar architecture (Figures E1A–E1D), the findings for the lungs of BLM-treated CAG mice showed that Col I–expressing cells were observed in a significant number of the cells in fibrotic lesions, in which scattered CD31–co-expressing cells could be identified. These findings suggested that endothelial-MT could be mediating the emergence of these cells at an intermediate stage between complete acquisition of mesenchymal phenotype and loss of endothelial markers.

Characterization of Lung Fibroblasts Derived from BLM-Treated CAG Mice

To directly prove the existence of endothelial-derived fibroblasts in BLM-induced lung fibrosis, lung fibroblasts from treated mice were evaluated for further studies. Lung fibroblasts from both saline- (SLF) and BLM-treated (BLF) mice were isolated, which in culture displayed the usual, primarily spindle-shaped fibroblast-like morphology. Upon X-gal staining, a few (3.1%) positive cells were identifiable in SLF cultures, while BLF cultures showed 16.2% to be positive (Figures 2A and 2B, respectively). To verify the fibroblastic nature or phenotype of the X-gal–positive fibroblast-like cells, BLFs were subjected to X-gal staining and sequentially followed by double immunocytochemical staining for Col I (Figure 2D, *red*) and α-SMA (Figure 2D, *green*). The results showed that the X-gal–positive BLFs consisted of two subpopulations: one that was both α-SMA– and Col I–positive (i.e., myofibroblastic), comprising 14.8% of X-gal–positive fibroblasts, and the other being α-SMA–negative but Col I–positive, comprising 85.2% of X-gal–positive fibroblasts (Figures 2C and 2D). It should be noted that X-gal–negative fibroblasts expressing α-SMA were also present, indicative of myofibroblasts not derived from endothelial cells. X-gal staining, followed by double immunostaining, for SLFs demonstrated that no or little α-SMA expression might be observed in X-gal–positive and –negative SLFs, although both SLFs exhibited Col I expression (Figures E2A and E2B). Both SLFs and BLFs were negative for CD31, indicating absence of contamination by endothelial cells in these cultured fibroblasts, or that all endothelial cell–derived fibroblasts had completely transitioned (data not shown). Thus significant numbers of fibroblasts from fibrotic lung were derived from endothelial cells, consistent with the occurrence of endothelial-MT in this model of pulmonary fibrosis.

A recent study showed that tissue endothelial cells might be derived from endothelial progenitor cells (EPC) in bone marrow (BM) (20), thus suggesting that not all endothelial cell–derived fibroblasts necessarily arise from local lung capillary endothelial cells. To evaluate the contribution of Tie2-expressing BM cells (versus local lung capillary endothelial cells) to X-gal–positive BLFs, BM chimeras were prepared by injection of BM cells collected from CAG mice or B6 mice into lethally irradiated CAG or B6 recipient mice. After stable engraftment was established, BLM-induced lung fibrosis was induced in the chimera mice. BLFs from CAG mice with the BM cells from B6 mice (B6 to CAG mice) showed 15.3% to be X-gal–positive (% of X-gal–positive cells; 15.3 ± 0.92 in BLFs from B6 to CAG mice). On the other hands, BLFs from B6 mice with BM from CAG mice (CAG to B6 mice) showed only 0.8% of X-gal–positive cells (% of X-gal–positive cells; 0.82 ± 0.15 in BLFs from B6 to CAG mice). SLFs from B6 to CAG mice or CAG to B6 mice yielded no or little of X-gal–positive fibroblasts (data not shown). Together, these findings demonstrated that the contribution of EPC in BM to endothelial cell–derived BLFs was minor, and that the predominant source appeared to be endogenous lung capillary endothelial cells via endothelial-MT.

Altered Expression of Endothelial-Specific Markers on Endothelial Cells by Combined Treatment with Activated Ras and TGF-β

To illuminate the underlying mechanism by which microvascular endothelial cells can undergo endothelial-MT *in vivo*, microvascular endothelial MS1 cells and the cells transduced with activated Ras gene (SVR cells) were used, since a previous report indicates that the combination of activated Ras and TGF-β treatment induces repression of epithelial phenotype such as E-cadherin expression in epithelial cells (21). These cells also allow us to eliminate the possibility of contribution by contaminating fibroblasts to the observations from further experiments, since these were derived from a single cell (22).

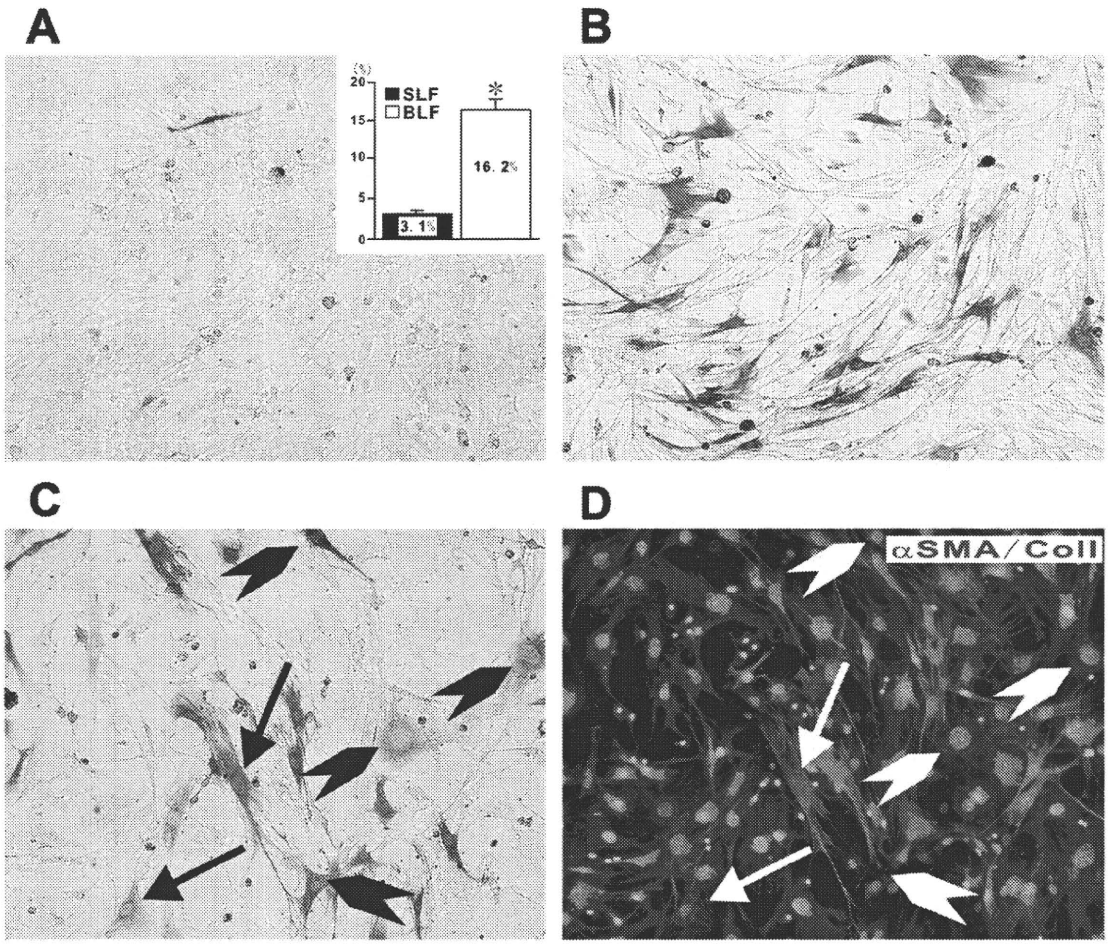

Figure 2. Characterization of BLM-induced lung fibroblasts derived from CAG mice. Saline-treated lung fibroblasts (SLF) or BLM-treated lung fibroblasts (BLF) derived from CAG mice were isolated and then stained with X-gal (SLF in *A* and BLF in *B*, respectively). The percentage of X-gal–positive cells among total counted cells, based on Hoechst 33342 nucleus staining, were shown in *inset* in *A*. Data shown in *inset* represent the means ± SEM from at least four samples (4 for SLF and 8 for BLF, respectively) in three independent experiments. Combined staining with X-gal and sequential immucytochemistry for Col I (*red*) and α-SMA (*green*) were performed for BLF derived from CAG mice (*C*, X-gal staining; *D*, immunocytochemistry for Col I and α-SMA, respectively). *Arrows* indicate X-gal (+)/Col I (+)/α-SMA (+) myofibroblasts. *Arrowheads* indicate X-gal (+)/Col I (+)/α-SMA (−) fibroblasts. A representative example of at least three independent experiments is shown. All images were photographed at ×200 magnification.

RT-PCR revealed that these endothelial cell lines expressed mRNAs for TGF-β receptor I and II (Figure 3A), thus suggesting that these cells would respond to TGF-β treatment. To evaluate the effect of these signals on endothelial cells, we examined the expression of endothelial-specific markers in response to combined treatment with activated Ras and TGF-β by FACS. Figures 3B and 3C showed that activated Ras signaling significantly repressed the expression of CD31, while TGF-β slightly inhibited expression, which was not statistically significant. However TGF-β caused significant repression of CD31 in the cells with activated Ras. On the other hand, Figures 3D and 3E showed that both activated Ras and TGF-β significantly repressed CD34 expression, although the effect of TGF-β was lower in magnitude relative to that of activated Ras alone. Nevertheless, combined treatment by these two agents significantly repressed the MFI for CD34 to 23% of that with vehicle treatment. Similar to the inhibitory pattern of CD31 expression, only the combination of activated Ras and TGF-β treatment caused significant repression of Tie2 expression (Figures 3F and E3A). TGF-β treatment of cells with activated Ras showed a significant repression of VE-cadherin expression, while activated Ras signaling slightly stimulated expression of VE-cadherin (Figures 3G and E3B). These data showed that although activated Ras alone caused significant repression of endothelial phenotype with the exception of VE-cadherin expression, combined treatment with TGF-β *in vitro* caused an additive steady repression of endothelial markers consistent with epithelial-MT (23).

Persistence of Altered Endothelial Phenotype in Ras-Activated Endothelial Cells after Withdrawal of TGF-β *In Vitro*

Epithelial-MT can be distinguished from "scattering," in which the phenotype changes are fully reversible after factor removal (21). In MS1 cells, the small but significant TGF-β–induced reduction in CD34 expression in the absence of activated Ras returned to normal levels upon TGF-β removal (Figures 4A and 4B). In contrast, the more robust TGF-β–induced suppression of CD34 expression in SVR cells with activated Ras, was persistent even up to 24 hours after TGF-β removal (Figures 4C and 4D). These findings would argue against the phenomena of scattering and instead would be consistent with endothelial-MT occurring in the cells exposed to activated Ras and TGF-β treatment.

De Novo Expression of Mesenchymal Phenotypes in Endothelial Cells by Combined Treatment with Activated Ras and TGF-β

Next, we evaluated whether combined treatment with activated Ras and TGF-β could yield gain of mesenchymal markers in endothelial cells. Fibronectin mRNA expression in endothelial cells treated with either TGF-β or activated Ras

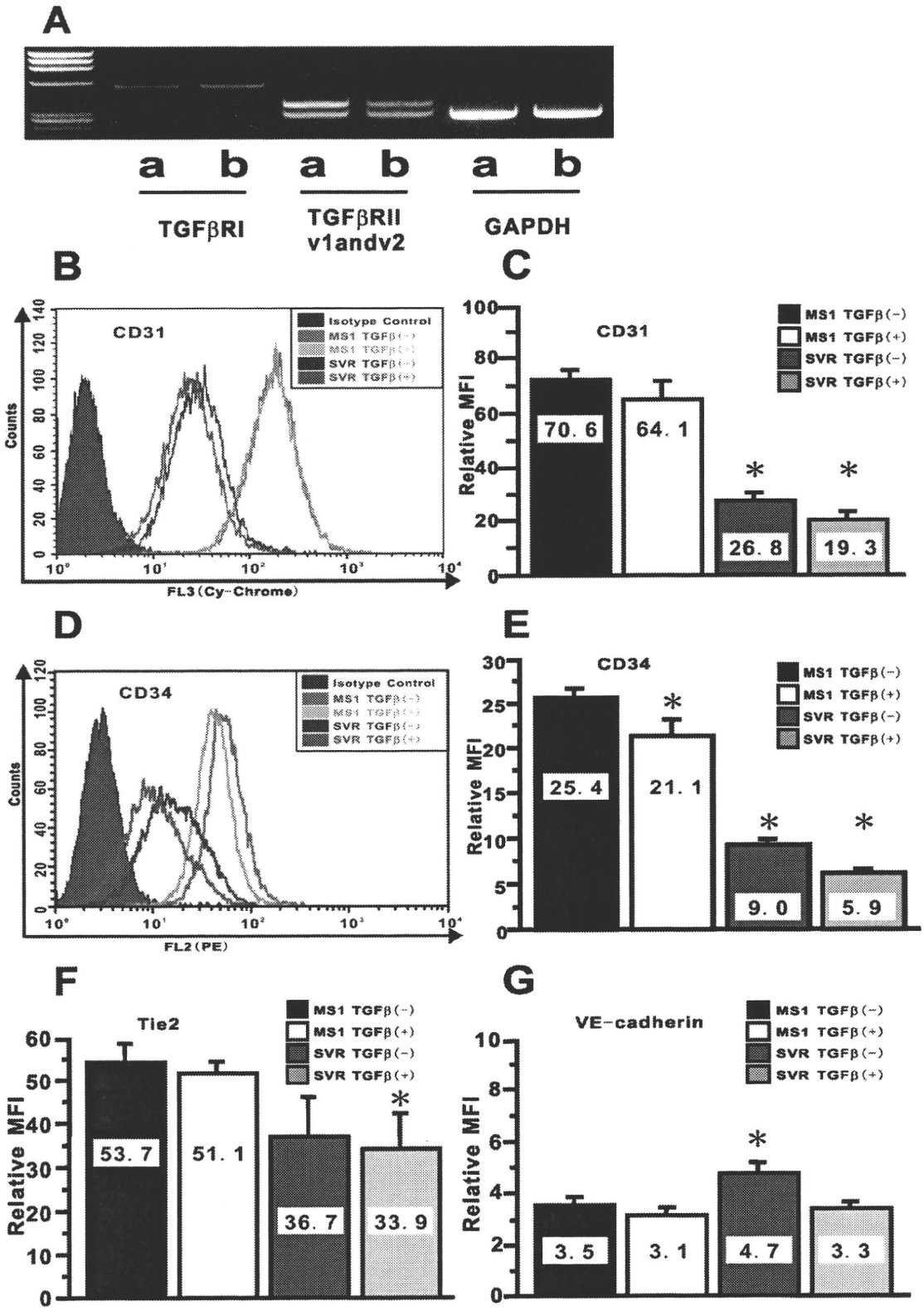

Figure 3. Altered expression of endothelial-specific markers by combined treatment with activated Ras and TGF-β. In *A*, the results of RT-PCR analysis for TGF-βRI, TGF-βRII variant1 (v1), variant2 (v2), and GAPDH are shown. Data shown are representative electropherograms of the indicated products using RNA samples from: MS1 (*lane a*) and SVR (*lane b*). These are representative of three independent experiments. CD31 in *B* and CD34 in *D* on endothelial MS1 and SVR treated with vehicle or TGF-β at 10 ng/ml for 24 hours were shown as overlaid histogram by FACS. The relative mean fluorescence intensity (MFI) for CD31 in *C*, for CD34 in *E*, for Tie2 in *F*, and for VE-cadherin in *G* were calculated as described in the online supplement. Data shown represent the means ± SEM from at least three independent experiments. *Asterisks* signify statistically significant difference ($P < 0.05$) in comparison with the relative MFI for each endothelial marker on MS1 with vehicle.

alone was significantly increased relative to that in untreated cells by 7.1-fold and 9.1-fold, respectively (Figure 5A). Treatment with both TGF-β and activated Ras caused a more dramatic induction of up to 20-fold increase over that of untreated cells (Figure 5A). Although an induction of Col I expression was observed upon treatment with TGF-β, constitutive activated Ras alone failed to significantly induce Col I expression. Combined treatment with both TGF-β and activated Ras yielded a more dramatic induction of up to 10-fold increase over that of untreated cells (Figure 5B). Next, we evaluated α-SMA expression in treated endothelial cells as an indicator of myofibroblast transdifferentiation. As expected, untreated endothelial cells did not express α-SMA, and neither did cells treated with either TGF-β or activated Ras

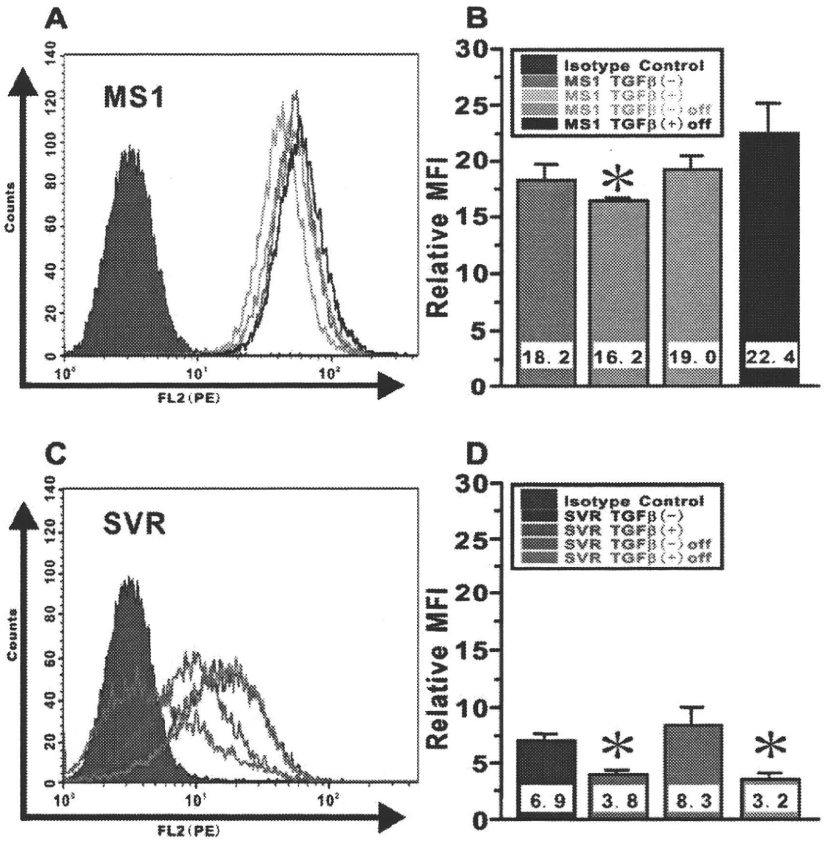

Figure 4. Persistence of altered endothelial phenotype in Ras-activated endothelial cells after withdrawal of TGF-β *in vitro*. Endothelial MS1 and SVR treated with vehicle or TGF-β at 10 ng/ml for 24 hours were cultured in complete medium after TGF-β removal for another 24 hours. CD34 expression on (*A*) MS1 cells and (C) SVR cells was shown as overlaid histogram by FACS. The relative MFI for CD34 in (*B*) MS1 cells and (*D*) SVR cells was calculated as described in the online supplement. Data shown represent the means ± SEM from at least three independent experiments. *Asterisks* signify statistically significant difference ($P < 0.05$) in comparison with the relative MFI for CD34 on MS1 or SVR with vehicle.

alone (Figures 5C–5E). In contrast, TGF-β treatment of cells with activated Ras induced significant morphological change and yielded cells exhibiting remarkable *de novo* α-SMA expression consistent with myofibroblast transdifferentiation (Figure 5F). Since the cells used in these experiments were derived from a single endothelial cell, a contribution to expression of these phenotypic markers from contaminating fibroblasts could be excluded. Interestingly, TGF-β treatment on the cells with activated Ras *in vitro* also caused significant induction of Snail and Twist, epithelial-MT–related transcription factors (Figures 5G and 5H).

Persistence of Endothelial-MT Phenotype in Ras-Activated Endothelial Cells after Withdrawal of TGF-β

After treatment of SVR cells with TGF-β to induce endothelial-MT, they were detached and replated in new dishes for culture in the absence of TGF-β. After 24 hours without TGF-β, the cells appeared to maintain their morphology and organized in a monolayer with occasional compact circular aggregates. TGF-β treatment of cells with activated Ras did not induce apoptosis (data not shown). To confirm that these complete endothelial-MT (cEMT) cells could maintain this endothelial-MT phenotype even after withdrawal of TGF-β, they were assessed by FACS for expression of endothelial markers. Compared with the basal expression of endothelial cells markers (Figures 3B, 3D, E3A, and E3B), the results showed that culturing in the absence of TGF-β did not reverse the endothelial-MT–associated significant reduction in expression of the endothelial markers CD31, Tie2, and VE-cadherin, although CD34 expression on a few cEMT cells appeared to revert back to the basal level (Figures 6A–6D). However, re-treatment with TGF-β significantly and stably repressed CD34 expression on cEMT cells (MFI in cEMT cells; 10.3, MFI in cEMT cell with TGF-β; 6.3, respectively). Thus, once activated Ras-transduced endothelial cells were treated with TGF-β, loss of endothelial phenotype was persistent even after withdrawal of exogenous TGF-β stimulation.

In contrast analysis of mesenchymal cell markers revealed that the TGF-β induction of fibronectin and Col I expression in cEMT cells was reversible (Figures 6E and 6F). Thus, when cultured in TGF-β–free media, the fibronectin and Col I mRNA levels in cEMT cells reverted back to levels seen in SVR cells before TGF-β stimulation (Figures 5A and 5B). However, when these cEMT cells were re-stimulated with TGF-β, the mRNA levels of both fibronectin and Col I were markedly induced to levels (Figures 6E and 6F) that were more than 2-fold higher than the levels achieved by the initial treatment with TGF-β (Figures 5A and 5B). These data suggested that cEMT cells had stably acquired a potential to produce abundant extracellular matrix (ECM) constituents such as fibronectin and Col I in response to TGF-β stimulation, a property that would be consistent with a fibroblast phenotype. cEMT cells maintained high levels of Snail and Twist expression, which could be further stimulated by re-treatment with TGF-β (Figures 6G and 6H).

In Vivo Acquisition of Endothelial-MT Phenotype in Ras-Activated Endothelial Cells

To evaluate whether endothelial cells could acquire endothelial-MT phenotype *in vivo*, MS1 or SVR cells were inoculated into the flank of nude mice with BALB/C background. At Day 28 after inoculation, primary tumors were established only in the group of SVR-treated nude mice, while only local hemangioma was detected in the group of MS1-treated nude mice even as

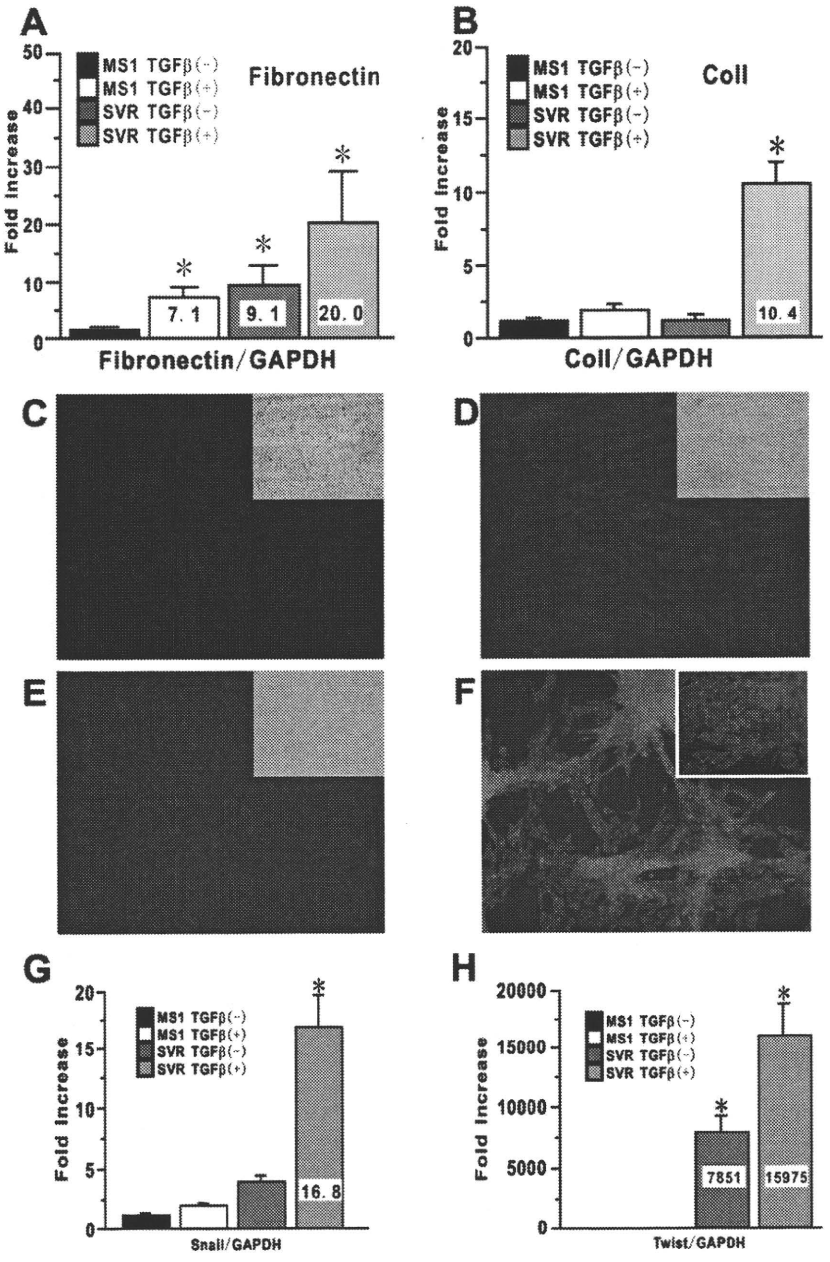

Figure 5. *De novo* induced expression of mesenchymal-specific markers in endothelial cells by combined treatment with activated Ras and TGF-β. Mesenchymal markers expression in MS1 and SVR treated with vehicle or TGF-β at 10 ng/ml for 24 hours were evaluated. Fibronectin mRNA in *A* and Col I mRNA in *B* were analyzed using real-time PCR. Data shown represent the means ± SEM from three independent experiments. Cultured cells in an 8-well Lab-Tek Chamber Slide were also treated with vehicle or 10 ng/ml TGF-β in medium without FCS for 24 hours for immunocytochemistry for α-SMA. (*C–F*) Treated cells were stained with FITC-conjugated mouse anti-α-SMA antibody. (*C*) MS1 with vehicle. (*D*) MS1 with TGF-β. (*E*) SVR with vehicle. (*F*) SVR with TGF-β. *Magnification*: ×200. The *insets* in *C–E* shows the light microscopic appearance of treated cells treated with each condition. *Inset* in *F* shows the cells stained with isotype-matched control IgG for α-SMA. A representative example of at least three independent experiments is shown. Snail mRNA in *G* and Twist mRNA in *H* were also analyzed using real-time PCR. Data shown represent the means ± SEM from three independent experiments. *Asterisks* signify statistically significant difference ($P < 0.05$) in comparison with the quantitative value of targeted mRNA in MS1 with vehicle.

long as 3 months after inoculation (data not shown). Gross morphological analysis of H&E-stained lung tissue sections showed that lung metastasis was observed only in SVR-treated nude mice (Figure 7A). The SVR cells from primary tumor tissue were isolated using selection with neomycin. In preliminary experiments, we confirmed that cultured naïve fibroblasts from skin and lung tissues were completely eliminated with the neomycin selection at the concentration of 400 μg/ml within the 14-day culture period. Immunocytochemistry confirmed that isolated cells were positive for H-2Kb, consistent with original derivation of the MS1 and SVR cells from C57BL/6 mice (data not shown). Evaluation of endothelial markers by FACS revealed that most of the isolated *ex vivo* SVR cells did not expresss CD31 (93.5%), VE-cadherin (87.1%), or CD34 (65.4%) (Figures 7B–7E). This is in contrast to the original MS1 and SVR cells, which were mostly positive for all three markers. Evaluation of mesenchymal phenotypes by real-time PCR revealed significant expression of both fibronectin and Col I by *ex vivo* SVR cells, which was significantly stimulated by more than 2-fold upon treatment with TGF-β (Figures 7F and 7G). Furthermore, *ex vivo* SVR cells also maintained high levels of Snail and Twist expression, which could be further stimulated by re-treatment with TGF-β (data not shown). These findings suggested that the implanted cells had undergone endothelial-MT *in vivo* that is consistent with the behavior of these cells *in vitro*.

DISCUSSION

Classification of idiopathic interstitial pneumonias (IIPs) based on histopathological patterns has had a significant impact on the prediction of clinical course of patients with the various IIPs, when supported by other parameters such as demographic, physiologic, and radiologic assessment (24). Nevertheless, the outcome of treatment for IIPs, especially for IPF, remains unsatisfactory. An explanation for poor response to anti-

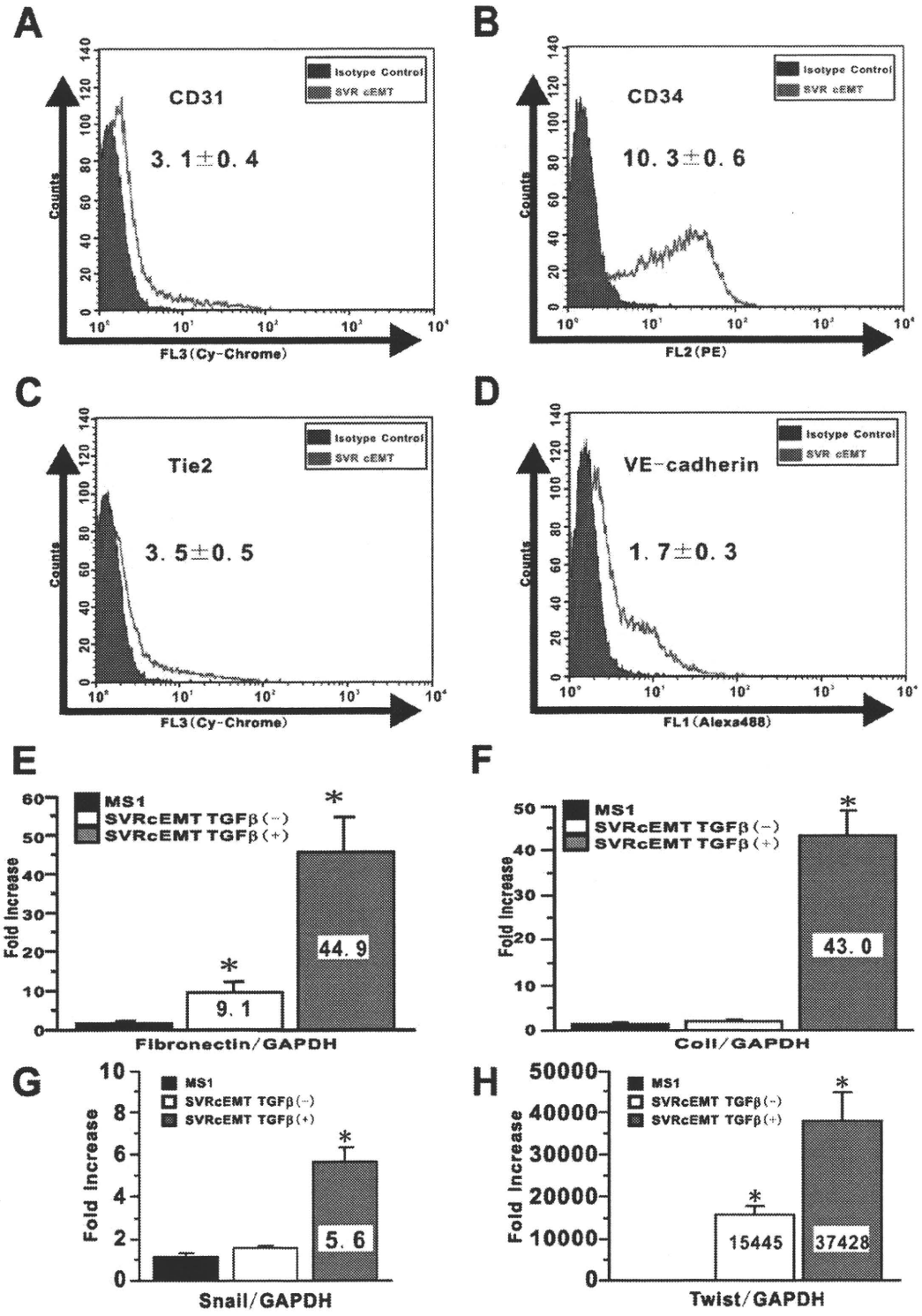

Figure 6. Persistence of endothelial-MT phenotype in Ras-activated endothelial cells after withdrawal of TGF-β. SVR treated with TGF-β were replated into the new culture dish and cultured with complete medium. The collected cells were called as cEMT cells. To evaluate whether cEMT cells can retain endothelial-MT phenotype or not, CD31 in *A*, CD34 in *B*, Tie-2 in *C*, and VE-cadherin expression in *D* on cEMT cells were shown as overlaid histogram by FACS. A representative example of at least three independent experiments is shown. Mesenchymal markers expressions in cEMT cells were also evaluated. Fibronectin mRNA in *E*, Col I mRNA in *F*, Snail mRNA in *G*, and Twist mRNA in *H* were analyzed using real-time PCR. Data shown represent the means ± SEM from three independent experiments. *Asterisks* signify statistically significant difference ($P < 0.05$) in comparison with the quantitative value of targeted mRNA in MS1.

inflammatory therapies for IPF is that extensive accumulation and/or proliferation of heterogeneous fibroblast populations may be a more important pathogenetic factor than the much lower level of inflammation seen in affected lung tissue (25). We have previously described the presence of BM-derived fibroblast-like cells, but not myofibroblasts, in injured lungs undergoing pulmonary fibrosis (4). In this present study, the possibility that lung capillary endothelial cells could serve as another source for fibroblasts in BLM-induced pulmonary fibrosis was examined. While there is no completely satisfactory animal model of human IPF, the BLM-induced model is relatively well-characterized and does exhibit certain features found in the human disease (26). Elucidation of the cellular origin of fibroblast in the context of remodeling/fibrosis on the one hand, and the biology of the various fibroblast subpopulations on the other, has the potential to revolutionize the treatment of patients with lung disorders such as IPF, emphysema, and other fibrotic lung diseases (27). It is assumed that combined stimulations for epithelial-MT might induce the persistent repression of the promoter activity of epithelial

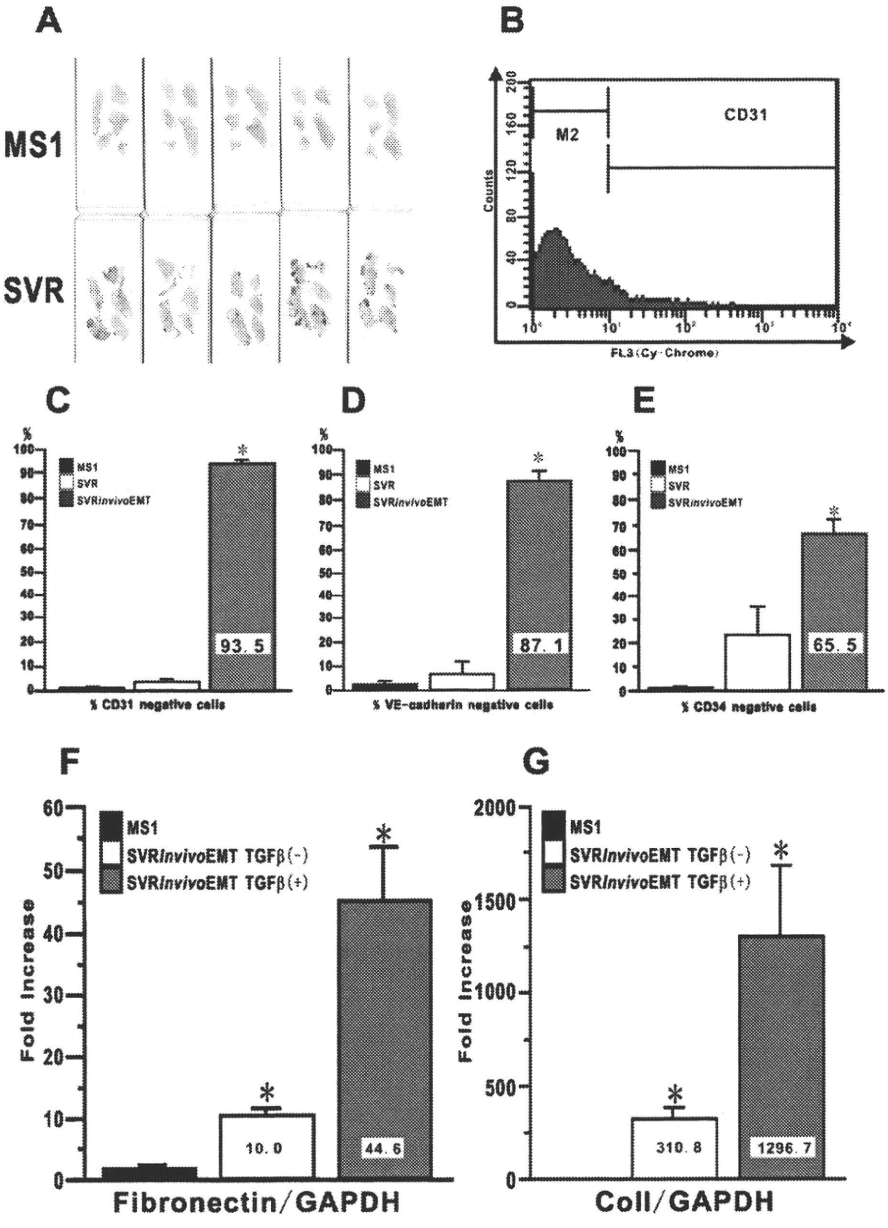

Figure 7. *In vivo* acquisition of endothelial-MT phenotype in Ras-activated endothelial cells. A quantity of 1×10^6 cells of MS1 or SVR were inoculated subcutaneously into the flank of nude mice. (*A*) The lungs from MS1-treated mice (*upper row*; $n = 5$) and SVR-treated mice (*lower row*; $n = 5$) were collected at Day 28 to evaluate lung metastasis. Collected primary tumors of SVR were digested and selected with neomycin. Selected *ex vivo* SVR cells, which we called *in vivo* EMT cells, were analyzed for the expression of endothelial-specific markers by FACS. (*B*) We defined the population of cells in M2 gate as marker-negative cells. The percentage of marker-negative cells for (C) CD31, (*D*) VE-cadherin, and (*E*) CD34 are shown. Data shown represent the means ± SEM from three independent experiments. Fibronectin mRNA in *F* and Col I mRNA in *G* were analyzed using real-time PCR. Data shown represent the means ± SEM from three independent experiments. *Asterisks* signify statistically significant difference ($P < 0.05$) in comparison with the quantitative value of targeted endothelial markers and mRNA in MS1.

markers, rather than its activation, resulting in persistent loss of epithelial markers (7, 8). Together with these reviews (7, 8), our present findings *in vitro* indicate that these stimulations for endothelial-MT might yield the repression of the promoter activity of endothelial markers and sequentially the vanishing endothelial markers expression in fibrosis model *in vivo*. Therefore, to confirm that endogenous endothelial cells *in vivo* could significantly contribute to the fibroblast population in lung fibrosis, we generated CAG mice, in which the activation of Cre recombinase under the control of the Tie2 promoter/enhancer induced the deletion of the CAT gene and consequently *de novo* irreversible LacZ gene expression in pan-endothelial cells, independent of the status of Tie2 promoter activity (28). X-gal staining of lungs from these double transgenic mice not only exhibited the expected distribution of Cre-mediated *de novo* LacZ expression in lung capillary endothelial cells under physiologic conditions, but also enable us to trace LacZ expressing endothelial-derived fibroblasts in the lungs of these mice under normal and/or pathological conditions. In control saline-treated mice, the distribution of LacZ expression in pulmonary capillary endothelial cells was clearly evident, similar to that seen in other studies of lung endothelial cells using Tie2-LacZ transgenic mice (29) as well as the distribution of Tie2 receptor in a study of idiopathic pulmonary hypertension (30). Thus our data indicated that Cre-mediated recombination in the lung occurred only in the intended cell type, namely the endothelial cell, with no detectable activity in other cell types, as other studies demonstrated using Tie2-Cre/ROSA26R mice (28, 31, 32). In contrast to the control lungs, those from BLM-injured CAG mice exhibited distorted morphology with extensive remodeling and vastly increased numbers of both X-gal–positive and –negative cells, virtually all densely clustered in areas undergoing active fibrosis. The extravascular and interstitial localization of some of these cells, and their morphology were consistent with interstitial mesenchymal cells, such as fibroblasts. As recent study with a surfactant protein C–driven Cre/loxP reporter system suggested that there were some epithelial cells with mesenchymal nature

as early epithelial-MT stage in lung fibrosis (6), our double immunostaining for CD31 and Col I showed that fibrotic lesions involved substantial numbers of fibroblast-like cells positive for Col I, some of which expressed CD31, indicating to be under intermediate state of endothelial-MT. Since it was difficult, if not impossible, in lung tissue sections to distinguish X-gal–positive endothelial-derived fibroblasts from X-gal–positive endothelial cells amid the distorted architecture of the remodeling lung tissue with collapse of the alveolar space, lung fibroblasts were isolated for further studies. Cultured fibroblasts from the lungs of BLM-treated CAG mice revealed mostly typical spindle-shaped fibroblast morphology similar to previously cultured primary murine lung fibroblasts (14). X-gal staining of fibroblast cultures from BLM-treated mice revealed that 16.2% of cells were LacZ-positive, which also expressed Col I and have typical fibroblast morphology. Of this LacZ-positive population, less than 15% of them expressed α-SMA, indicating that only a small minority of endothelial cell–derived cells was able to differentiate to myofibroblasts. A much smaller (3.1%) proportion were LacZ-positive in cells isolated from saline-treated animals, probably due to basal contribution of endothelial-derived fibroblasts under physiological condition. The finding that both SLFs and BLFs were negative for CD31 in our fibroblasts culture system might be supported by the previous study (33) and also explained by the manufacturer's recommendations that many kinds of growth factors are usually needed to keep primary cultured endothelial cells *in vitro* (34). Recent lineage tracking analysis in combination with a Tie2-driven Cre/loxP reporter system suggested that only 1–5% of the endothelium in liver may be derived from BM-derived EPC (35). Furthermore, Zeisberg and coworkers also evaluated a lesser contribution by BM-derived cells in endothelial-derived fibroblasts in cardiac fibrosis using the Tie1-driven Cre/loxP reporter system (36). Our finding that BM-derived cells did not substantially contribute to the X-gal–positive BLFs in our lung fibrosis model was compatible with these previous studies (35, 36). These novel findings for the first time directly demonstrated that lung endothelial cells in BLM-induced fibrotic lungs could give rise to significant numbers of fibroblasts, while possible existence of nonendothelial resident lung Tie-2–positive progenitors could not be completely excluded.

To illuminate the underlying mechanism, by which "micro"-vascular endothelial cells can undergo endothelial-MT *in vivo*, we used the "micro"-vascular endothelial cell line MS1 cells and SVR cells, derived as a single cell clone using different drug selections, respectively (22). Although there are clear limitations to these "micro"-vascular endothelial cell lines in terms of tissue derivation from pancreatic islets, they remain useful for tracking endothelial-MT *in vitro*, since it allows us to eliminate the possibility of contribution by contaminating fibroblasts to the observations from experiments using these cells derived from a single clone. A recent review by Thiery and Sleeman suggested that the exact mechanisms remain unclear, although complex network of multiple signaling pathways organizes epithelial-MT process in epithelial lineages (8). In this study we showed that the combination of activated Ras and TGF-β treatment *in vitro* induced stable repression of endothelial markers reminiscent of endothelial-MT. Although the inability of TGF-β treatment alone to repress CD31 expression is also noted in aortic valve endothelial cells *in vitro* (37), a study using a hepatocyte cell line suggests that the expression of the junctional proteins remained unaffected or little changed during the first 24 hours, but progressively decreased after prolonged TGF-β treatment (38). Our finding that endothelial phenotypic changes in MS1 cells without an activated Ras gene were resistant to repressive effect of TGF-β treatment alone on endothelial markers (aside from CD34 expression), was compatible with these previous studies (37, 38). In our latter experiment, loss of endothelial phenotypes such as CD31, CD34, VE-Cadherin, and Tie2 was observed in endothelial cells after the completion of endothelial-MT (referred to as cEMT). These findings suggested that more rapid repression of CD34 expression than that of CD31 expression might depend on the differential response to combined signaling with activated Ras and TGF-β.

Growth factors such as FGF, HGF, or TGF-β alone are known to have scattering factor activity, which is reversible (i.e., upon their removal the growth factor-induced phenotype changes are fully reversible) (21). Our findings in endothelial cells are consistent with this report in that TGF-β treatment alone induced only the reversible "scattering" phenotype without any morphological change. In contrast, TGF-β treatment in combination with activated Ras gave rise to persistent repression of endothelial markers even after TGF-β removal.

Another essential characteristic of epithelial-MT is gain or *de novo* expression of mesenchymal markers (39). Fibronectin and Col I are the most critical ECM constituents in lung fibrosis. Fibronectin expression was increased 20-fold in SVR cells treated with TGF-β, compared with untreated endothelial (MS1) cells in our study. Although untreated MS1 cells exhibited no or little expression of Col I mRNA, the *de novo* expression of Col I was markedly induced in TGF-β–treated endothelial cells with activated Ras, up to 10-fold increase over that of untreated cells. A marker of myofibroblast differentiation that is often used is α-SMA expression (40). Our previous report showed the unexpected finding that BM-derived fibroblasts do not give rise to α-SMA–expressing myofibroblasts, even after *in vitro* TGF-β stimulation, indicating that the BM is not a significant source of progenitor cells for myofibroblasts in injured lung undergoing fibrosis (4). Previous reports indicate that *de novo* α-SMA expression could be induced in "macro"-vascular endothelial cells by prolonged (from 6–28 d) treatment with TGF-β alone (37, 41), but interestingly, not in "micro"-vascular endothelial cells (41). In our study, only the combination of activated Ras and TGF-β treatment could induce *de novo* α-SMA expression in "micro"-vascular endothelial cells, while neither activated Ras nor TGF-β alone was able to induce α-SMA expression. Triggering epithelial-MT is known to result in the activation of transcriptional regulators such as Snail and Twist, which regulate the changes in gene expression patterns that underlie epithelial-MT (8). In our study, substantial induction of Snail and Twist in endothelial cells treated with activated Ras and TGF-β seemed to be compatible with these findings, consistent with their importance during endothelial-MT as well.

Loss of endothelial phenotype after the completion of endothelial-MT (we called cEMT) appeared stable and irreversible since cessation of exogenous TGF-β treatment did not cause reversion to the endothelial phenotype. In addition, upon re-treatment with TGF-β, cEMT cells exhibited the potential for significantly higher levels of ECM expression compared with that in cells responding to initial treatment with TGF-β. These findings were supported with significantly increasing Snail and Twist expression in cEMT cells, compared with those observed in endothelial cells.

As previously reported (22), SVR with activated Ras, but not MS1 cells, caused tumors in the flank of nude mice. All nude mice with primary tumors of SVR endothelial cells also exhibited gross lung metastasis. There is accumulating evidence to indicate that epithelial-MT may be involved in tumor metastasis (8). In our study, neomycin-selected *ex vivo* SVR cells exhibited evidence of undergoing endothelial-MT *in vivo*,

probably due to stimulation by endogenous TGF-β derived from tumor-associated cells or fibroblasts (42), and subsequently caused or promoted the distant metastasis observed in the lung. Although several studies suggest the possibility of myofibroblast-like cells being derived from primary "macro"-vascular endothelial cells (12, 43), our comprehensive evaluation for altered phenotypes in the endothelial cells derived from a single cell is the first to directly show that "micro"-vascular endothelial cells could undergo endothelial-MT *in vitro* by combination of activated Ras and TGF-β treatment. These findings using microvascular endothelial cell line *in vitro* allow us to speculate that the underlying mechanism by which capillary endothelial cell in BLM-treated lungs could yield another population of fibroblasts might be an endothelial-MT process, most likely under the influence of both TGF-β and growth factors capable of activating the Ras/MAPK pathway, which are known to be elaborated by both recruited and resident cells in fibrotic lesions (44).

Our previous study using GFP BM chimera mice demonstrated that α-SMA–expressing myofibroblasts appeared not to be of BM origin, and more likely originating from peribronchial and perivascular adventitial fibroblasts or other intrapulmonary precursor cells (4, 45). Our present finding suggested the endothelial cell as one of the candidate intrapulmonary precursor cell for the myofibroblast in lung fibrosis. The histopathology of IPF indicates increased capillary density around fibroblastic foci with evidence of vascular regression in the center of these foci (46). One interpretation for this vascular heterogeneity may be due to an inability to form new vessels in areas of established fibrosis and inhibition of angiogenesis (46, 47). Our evidence of transition of endothelial cells into fibroblasts through endothelial-MT in BLM-induced lung fibrosis provides an alternative explanation by suggesting that the basis for the vascular regression may be the loss of endothelial cells via endothelial-MT to contribute to the fibroblastic elements in these foci. Pulmonary vascular remodeling in IPF-associated pulmonary hypertension (PH), as one of the most critical complications, represents not only pathological and biological endothelial loss but also the neointima formation with α-SMA–expressing mesenchymal cells and ECM beneath a dysfunctional endothelial layer, both of which are assumed to be common features in idiopathic pulmonary hypertension and atherosclerosis (48, 49). Futhermore, the question of their potential myofibroblastic nature has been suggested from comprehensive analysis for α-SMA–expressing mesenchymal cells in atherosclerosis, although smooth muscle cells (SMCs) originating from media have been assumed to contribute to α-SMA–expressing mesenchymal cells in neointima (40, 48). Sumioka and coworkers as well as Zeisberg and colleagues suggested the possibility of endothelial-derived fibroblasts in cardiac, kidney, and eye fibrosis (36, 50, 51) and carcinoma as well (52). Further investigation into endothelial-derived fibroblasts/myofibroblasts in the pathogenesis of not only pulmonary vascular remodeling in IPF-associated PH, but also neointima formation in atherosclerosis, is warranted.

In summary, we confirmed that endogenous lung endothelial cells in intact animals could also give rise to significant numbers of fibroblasts in a murine model of bleomycin-induced lung injury and fibrosis. The underlying mechanism was suggested by *in vitro* studies showing that endothelial-MT could occur in endothelial cell lines when treated with TGF-β in combination with activation of Ras signaling. Furthermore, this same cell line could undergo a similar transition to fibroblasts *in vivo* when implanted in nude mice.

Author Disclosure: None of the authors has a financial relationship with a commercial entity that has an interest in the subject of this manuscript.

References

1. Gross TJ, Hunninghake GW. Idiopathic pulmonary fibrosis. *N Engl J Med* 2001;345:517–525.
2. Thannickal VJ, Toews GB, White ES, Lynch JP III, Martinez FJ. Mechanisms of pulmonary fibrosis. *Annu Rev Med* 2004;55:395–417.
3. Iwano M, Plieth D, Danoff TM, Xue C, Okada H, Neilson EG. Evidence that fibroblasts derive from epithelium during tissue fibrosis. *J Clin Invest* 2002;110:341–350.
4. Hashimoto N, Jin H, Liu T, Chensue SW, Phan SH. Bone marrow-derived progenitor cells in pulmonary fibrosis. *J Clin Invest* 2004;113: 243–252.
5. Willis BC, Liebler JM, Luby-Phelps K, Nicholson AG, Crandall ED, du Bois RM, Borok Z. Induction of epithelial-mesenchymal transition in alveolar epithelial cells by transforming growth factor-beta1: potential role in idiopathic pulmonary fibrosis. *Am J Pathol* 2005;166:1321–1332.
6. Kim KK, Kugler MC, Wolters PJ, Robillard L, Galvez MG, Brumwell AN, Sheppard D, Chapman HA. Alveolar epithelial cell mesenchymal transition develops in vivo during pulmonary fibrosis and is regulated by the extracellular matrix. *Proc Natl Acad Sci USA* 2006; 103:13180–13185.
7. Grunert S, Jechlinger M, Beug H. Diverse cellular and molecular mechanisms contribute to epithelial plasticity and metastasis. *Nat Rev Mol Cell Biol* 2003;4:657–665.
8. Thiery JP, Sleeman JP. Complex networks orchestrate epithelial-mesenchymal transitions. *Nat Rev Mol Cell Biol* 2006;7:131–142.
9. Franks TJ, Colby TV, Travis WD, Tuder RM, Reynolds HY, Brody AR, Cardoso WV, Crystal RG, Drake CJ, Engelhardt J, *et al.* Resident cellular components of the human lung: current knowledge and goals for research on cell phenotyping and function. *Proc Am Thorac Soc* 2008;5:763–766.
10. Dutly AE, Andrade CF, Verkaik R, Kugathasan L, Trogadis J, Liu M, Waddell TK, Stewart DJ, Keshavjee S. A novel model for post-transplant obliterative airway disease reveals angiogenesis from the pulmonary circulation. *Am J Transplant* 2005;5:248–254.
11. Frid MG, Kale VA, Stenmark KR. Mature vascular endothelium can give rise to smooth muscle cells via endothelial-mesenchymal transdifferentiation: in vitro analysis. *Circ Res* 2002;90:1189–1196.
12. Arciniegas E, Frid MG, Douglas IS, Stenmark KR. Perspectives on endothelial-to-mesenchymal transition: potential contribution to vascular remodeling in chronic pulmonary hypertension. *Am J Physiol Lung Cell Mol Physiol* 2007;293:L1–L8.
13. Sakai K, Miyazaki J. A transgenic mouse line that retains Cre recombinase activity in mature oocytes irrespective of the cre transgene transmission. *Biochem Biophys Res Commun* 1997;237:318–324.
14. Huaux F, Liu T, McGarry B, Ullenbruch M, Phan SH. Dual roles of IL-4 in lung injury and fibrosis. *J Immunol* 2003;170:2083–2092.
15. Hashimoto N, Kawabe T, Hara T, Imaizumi K, Wakayama H, Saito H, Shimokata K, Hasegawa Y. Effect of erythromycin on matrix metalloproteinase-9 and cell migration. *J Lab Clin Med* 2001;137:176–183.
16. Yuan Q, Austen KF, Friend DS, Heidtman M, Boyce JA. Human peripheral blood eosinophils express a functional c-kit receptor for stem cell factor that stimulates very late antigen 4 (VLA-4)-mediated cell adhesion to fibronectin and vascular cell adhesion molecule 1 (VCAM-1). *J Exp Med* 1997;186:313–323.
17. Noguchi M, Imaizumi K, Kawabe T, Wakayama H, Horio Y, Sekido Y, Hara T, Hashimoto N, Takahashi M, Shimokata K, *et al.* Induction of antitumor immunity by transduction of CD40 ligand gene and interferon-gamma gene into lung cancer. *Cancer Gene Ther* 2001;8: 421–429.
18. Hashimoto N, Kawabe T, Imaizumi K, Hara T, Okamoto M, Kojima K, Shimokata K, Hasegawa Y. CD40 plays a crucial role in lipopolysaccharide-induced acute lung injury. *Am J Respir Cell Mol Biol* 2004;30:808–815.
19. Livak KJ, Schmittgen TD. Analysis of relative gene expression data using real-time quantitative PCR and the 2(-Delta Delta C(T)) Method. *Methods* 2001;25:402–408.
20. Asahara T, Murohara T, Sullivan A, Silver M, van der Zee R, Li T, Witzenbichler B, Schatteman G, Isner JM. Isolation of putative progenitor endothelial cells for angiogenesis. *Science* 1997;275:964–967.
21. Janda E, Lehmann K, Killisch I, Jechlinger M, Herzig M, Downward J, Beug H, Grunert S. Ras and TGF[beta] cooperatively regulate epithelial cell plasticity and metastasis: dissection of Ras signaling pathways. *J Cell Biol* 2002;156:299–313.
22. Arbiser JL, Moses MA, Fernandez CA, Ghiso N, Cao Y, Klauber N, Frank D, Brownlee M, Flynn E, Parangi S, *et al.* Oncogenic H-ras

stimulates tumor angiogenesis by two distinct pathways. *Proc Natl Acad Sci USA* 1997;94:861–866.
23. Gotzmann J, Huber H, Thallinger C, Wolschek M, Jansen B, Schulte-Hermann R, Beug H, Mikulits W. Hepatocytes convert to a fibroblastoid phenotype through the cooperation of TGF-beta1 and Ha-Ras: steps towards invasiveness. *J Cell Sci* 2002;115:1189–1202.
24. Flaherty KR, Andrei AC, Murray S, Fraley C, Colby TV, Travis WD, Lama V, Kazerooni EA, Gross BH, Toews GB, *et al.* Idiopathic pulmonary fibrosis: prognostic value of changes in physiology and six-minute-walk test. *Am J Respir Crit Care Med* 2006;174:803–809.
25. Sheppard D. Pulmonary fibrosis: a cellular overreaction or a failure of communication? *J Clin Invest* 2001;107:1501–1502.
26. Liu T, Jin H, Ullenbruch M, Hu B, Hashimoto N, Moore B, McKenzie A, Lukacs NW, Phan SH. Regulation of found in inflammatory zone 1 expression in bleomycin-induced lung fibrosis: role of IL-4/IL-13 and mediation via STAT-6. *J Immunol* 2004;173:3425–3431.
27. Gharaee-Kermani M, Gyetko MR, Hu B, Phan SH. New insights into the pathogenesis and treatment of idiopathic pulmonary fibrosis: a potential role for stem cells in the lung parenchyma and implications for therapy. *Pharm Res* 2007;24:819–841.
28. Kisanuki YY, Hammer RE, Miyazaki J, Williams SC, Richardson JA, Yanagisawa M. Tie2-Cre transgenic mice: a new model for endothelial cell-lineage analysis in vivo. *Dev Biol* 2001;230:230–242.
29. Schlaeger TM, Bartunkova S, Lawitts JA, Teichmann G, Risau W, Deutsch U, Sato TN. Uniform vascular-endothelial-cell-specific gene expression in both embryonic and adult transgenic mice. *Proc Natl Acad Sci USA* 1997;94:3058–3063.
30. Dewachter L, Adnot S, Fadel E, Humbert M, Maitre B, Barlier-Mur AM, Simonneau G, Hamon M, Naeije R, Eddahibi S. Angiopoietin/Tie2 pathway influences smooth muscle hyperplasia in idiopathic pulmonary hypertension. *Am J Respir Crit Care Med* 2006;174:1025–1033.
31. Koni PA, Joshi SK, Temann UA, Olson D, Burkly L, Flavell RA. Conditional vascular cell adhesion molecule 1 deletion in mice: impaired lymphocyte migration to bone marrow. *J Exp Med* 2001;193:741–754.
32. Limbourg FP, Takeshita K, Radtke F, Bronson RT, Chin MT, Liao JK. Essential role of endothelial Notch1 in angiogenesis. *Circulation* 2005;111:1826–1832.
33. Whiting CV, Tarlton JF, Bailey M, Morgan CL, Bland PW. Abnormal mucosal extracellular matrix deposition is associated with increased TGF-beta receptor-expressing mesenchymal cells in a mouse model of colitis. *J Histochem Cytochem* 2003;51:1177–1189.
34. Takagi Y, Hashimoto N, Phan SH, Imaizumi K, Matsuo M, Nakashima H, Hashimoto I, Hayashi Y, Kawabe T, Shimokata K, *et al.* Erythromycin-induced CXCR4 expression on microvascular endothelial cells. *Am J Physiol Lung Cell Mol Physiol* 2009;297:L420–L431.
35. Bailey AS, Willenbring H, Jiang S, Anderson DA, Schroeder DA, Wong MH, Grompe M, Fleming WH. Myeloid lineage progenitors give rise to vascular endothelium. *Proc Natl Acad Sci USA* 2006;103:13156–13161.
36. Zeisberg EM, Tarnavski O, Zeisberg M, Dorfman AL, McMullen JR, Gustafsson E, Chandraker A, Yuan X, Pu WT, Roberts AB, *et al.* Endothelial-to-mesenchymal transition contributes to cardiac fibrosis. *Nat Med* 2007;13:952–961.
37. Paranya G, Vineberg S, Dvorin E, Kaushal S, Roth SJ, Rabkin E, Schoen FJ, Bischoff J. Aortic valve endothelial cells undergo transforming growth factor-beta-mediated and non-transforming growth factor-beta-mediated transdifferentiation in vitro. *Am J Pathol* 2001;159:1335–1343.
38. Gotzmann J, Fischer AN, Zojer M, Mikula M, Proell V, Huber H, Jechlinger M, Waerner T, Weith A, Beug H, *et al.* A crucial function of PDGF in TGF-beta-mediated cancer progression of hepatocytes. *Oncogene* 2006;25:3170–3185.
39. Kalluri R, Neilson EG. Epithelial-mesenchymal transition and its implications for fibrosis. *J Clin Invest* 2003;112:1776–1784.
40. Hinz B, Phan SH, Thannickal VJ, Galli A, Bochaton-Piallat ML, Gabbiani G. The myofibroblast: one function, multiple origins. *Am J Pathol* 2007;170:1807–1816.
41. Paruchuri S, Yang JH, Aikawa E, Melero-Martin JM, Khan ZA, Loukogeorgakis S, Schoen FJ, Bischoff J. Human pulmonary valve progenitor cells exhibit endothelial/mesenchymal plasticity in response to vascular endothelial growth factor-A and transforming growth factor-beta2. *Circ Res* 2006;99:861–869.
42. Orimo A, Gupta PB, Sgroi DC, Arenzana-Seisdedos F, Delaunay T, Naeem R, Carey VJ, Richardson AL, Weinberg RA. Stromal fibroblasts present in invasive human breast carcinomas promote tumor growth and angiogenesis through elevated SDF-1/CXCL12 secretion. *Cell* 2005;121:335–348.
43. Arciniegas E, Neves CY, Carrillo LM, Zambrano EA, Ramirez R. Endothelial-mesenchymal transition occurs during embryonic pulmonary artery development. *Endothelium* 2005;12:193–200.
44. Chapman HA. Disorders of lung matrix remodeling. *J Clin Invest* 2004;113:148–157.
45. Zhang K, Rekhter MD, Gordon D, Phan SH. Myofibroblasts and their role in lung collagen gene expression during pulmonary fibrosis: a combined immunohistochemical and in situ hybridization study. *Am J Pathol* 1994;145:114–125.
46. Ebina M, Shimizukawa M, Shibata N, Kimura Y, Suzuki T, Endo M, Sasano H, Kondo T, Nukiwa T. Heterogeneous increase in CD34-positive alveolar capillaries in idiopathic pulmonary fibrosis. *Am J Respir Crit Care Med* 2004;169:1203–1208.
47. Renzoni EA. Neovascularization in idiopathic pulmonary fibrosis: too much or too little? *Am J Respir Crit Care Med* 2004;169:1179–1180.
48. Hao H, Gabbiani G, Camenzind E, Bacchetta M, Virmani R, Bochaton-Piallat ML. Phenotypic modulation of intima and media smooth muscle cells in fatal cases of coronary artery lesion. *Arterioscler Thromb Vasc Biol* 2006;26:326–332.
49. Nathan SD, Noble PW, Tuder RM. Idiopathic pulmonary fibrosis and pulmonary hypertension: connecting the dots. *Am J Respir Crit Care Med* 2007;175:875–880.
50. Sumioka T, Ikeda K, Okada Y, Yamanaka O, Kitano A, Saika S. Inhibitory effect of blocking TGF-beta/Smad signal on injury-induced fibrosis of corneal endothelium. *Mol Vis* 2008;14:2272–2281.
51. Zeisberg EM, Potenta SE, Sugimoto H, Zeisberg M, Kalluri R. Fibroblasts in kidney fibrosis emerge via endothelial-to-mesenchymal transition. *J Am Soc Nephrol* 2008;19:2282–2287.
52. Zeisberg EM, Potenta S, Xie L, Zeisberg M, Kalluri R. Discovery of endothelial to mesenchymal transition as a source for carcinoma-associated fibroblasts. *Cancer Res* 2007;67:10123–10128.